Pergamon

Geochimica et Cosmochimica Acta, Vol. 62, No. 1, pp. 89–108, 1998
Copyright © 1998 Elsevier Science Ltd
Printed in the USA. All rights reserved
0016-7037/98 $19.00 + .00

PII S0016-7037(97)00319-0

Geochemical and neutronic characteristics of the natural fossil fission reactors at Oklo and Bangombé, Gabon

HIROSHI HIDAKA*,[1] AND PHILIPPE HOLLIGER[2]

[1]Department of Earth and Planetary Systems Science, Hiroshima University, Higashi-Hiroshima 739, Japan
[2]Department of Optronics, Commissariat à l'Energie Atomique, 38054 Grenoble Cedex 9, France

(*Received March* 6, 1996; *accepted in revised form September* 2, 1997)

Abstract—Isotopic studies have been completed on samples from the natural fission reactors at Oklo and Bangombé in order to determine the conditions under which they functioned when critical and to evaluate the retention and migration of fissiogenic radionuclides. The abundances and isotopic compositions of the elements Rb, Sr, Zr, Ru, Pd, Ag, Te, Ba, rare earth elements (REEs), and U have been measured by thermal ionization mass spectrometry (TIMS) and inductively coupled plasma mass spectrometry (ICP-MS). Isotopic analyses and in situ ion imaging have also been performed by using an ion microprobe. Seven samples were taken from the SF84 borehole (zone 10), one from the S2 borehole in gallery SD37 (zone 13), both being zones in the Oklo deposit, and one from the BA145 borehole in the Bangombé deposit. The isotopic data allow for a detailed description of the functional conditions of these reactors, and based on these results, we have calculated the retention rates of the fissiogenic nuclides and nucleogenic Bi and Th.

The nuclear parameters of the natural fission reactors are characterized by the isotopic abundances of Ru, Nd, Sm, Gd, Er, Yb, Lu, and U: neutron fluence (n/cm^2), fission proportions of ^{235}U, ^{238}U, and ^{239}Pu, the restitution factor of ^{235}U resulting from ^{239}Pu decay, average temperature (°C) in the reactor, and duration of functioning (yr). In the 70 cm thick reactor core encountered by borehole SF84, the neutron fluence is in the range from 5.3×10^{20} to 8.0×10^{20} (n/cm^2). The variation in ^{235}U depletion shows a strong positive correlation with the restitution factor and an inverse correlation with neutron fluence, which demonstrates the stability of the reaction zone since the period of criticality. Large depletions of ^{149}Sm, ^{155}Gd, and ^{157}Gd have been detected in a sample of sandstone from 60 cm below this reactor core which also had a normal uranium isotopic ratio (^{235}U/^{238}U = 0.007254); this resulted from neutron capture reactions. The neutron fluence calculated from these isotopic anomalies is relatively high (6.2×10^{18} n/cm^2) and probably shows that nuclear reactions began, but that criticality could never be sustained due to an excess of neutron poisons (e.g., Sm and Gd). The results obtained from SD37 reveal that reactor zone 13 is not similar to the other reactor zones. The proportion of ^{238}U fission as calculated from the isotopic composition of Ru is extremely high (18% of the total), while that of SF84 (zone 10) is at most 5.0% of total fission. This result implies that the duration of criticality in reactor zone 13 was much shorter than in other reactor zones. In the Bangombé reactor zone BA145, the chemical and nuclear characteristics are close to those of SF84.

The retentivities of many fission products as compared with fissiogenic Nd have been assessed for the reactor core samples. From the measured and calculated relative retentions, more than 90% of fissiogenic Ru, Rh, Pd, Te, and REEs have been retained in SF84 and SD37. In these same zones, however, the relative retentions of fissiogenic alkaline and alkaline earth elements are less than 20%. The retentions of long-lived radioisotopes, such as ^{90}Sr, ^{99}Tc, ^{137}Cs, ^{236}U, and ^{237}Np have been calculated by reference to their radiogenic daughters ^{90}Zr, ^{99}Ru, ^{137}Ba, ^{232}Th, and ^{209}Bi, respectively. The excess or depletion of isotopic abundances measured in the daughter nuclides has allowed the prediction of the rate of chemical fractionation between the parent and daughter nuclides in the reactor during criticality. These results greatly improve the understanding of the Oklo phenomenon and provide important data for the evaluation of the concept of long-term storage of radioactive wastes in geological formations. *Copyright © 1998 Elsevier Science Ltd*

1. INTRODUCTION

The long-term retention of radionuclides in geological formations is of great concern in the isolation of radioactive waste. The study of natural analogues provides vital information on the geochemical behaviour of radionuclides over long periods. The Oklo uranium mine is now recognized as a unique natural analogue in which fission chain reactions occurred in uranium-rich sedimentary rocks 1.97 billion years ago (Holliger, 1993a; Gauthier-Lafaye et al., 1996). Since their discovery in 1972 (Bodu et al., 1972; Neuilly et al., 1972), sixteen reactor zones (hereafter referred to as RZs) have been identified in this deposit, as shown in Fig. 1. These RZs are numbered in their chronological order of discovery, and most of them still contain large quantities of fission products. Among them, RZs 10, 13, and 16 are of great interest owing to their depth, which has shielded them from surface alteration. They are seen in the mine at depths of 150–250 m, while RZs 1–9 and 15 were found during open pit mining. RZ 10 was discovered in 1982 (Gauthier-Lafaye et al., 1989a) during boring from one of the mine galleries and has frequently been encountered in subsequent borings and headings. RZ 13 was discovered in 1984; it is located from 10 to 30 m south of a dolerite dyke which intruded the strata 750 Ma ago (Nagy et al., 1991; Holliger,

*Author to whom correspondence should be addressed.

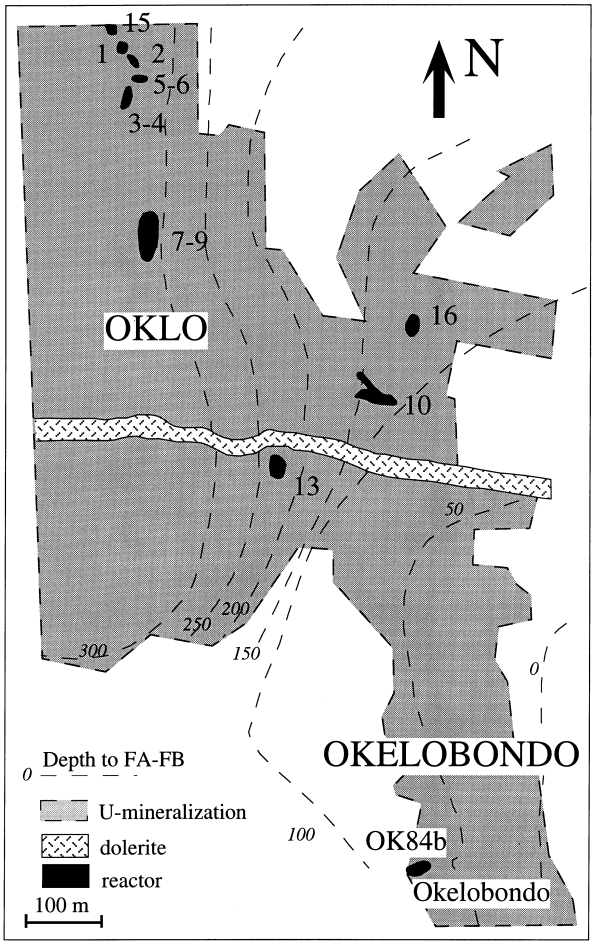

Fig. 1. The location of Oklo reactor zones. RZs 1–9 and 15 are located in the open pit at the northern part of Oklo. RZs 10–14 and 16 are located in the east and the south underground workings of the mine.

1992, 1994). In 1986 another RZ was discovered at Bangombé, 30 km to the southeast of Oklo. The RZ of the Bangombé deposit is nearer the surface (less than 12 m) than those at Oklo, and the overlying bed of pelite is thin and strongly altered (Toulhoat et al., 1994). The Bangombé RZ was identified from two adjacent boreholes. The location of the RZ and of recent drilling (BAX) at Bangombé is shown in Fig. 2. In 1990, the CEA (Commissariat a l'Energie Atomique) and CEC (Commission of European Communities) jointly started a program of research into the hydrogeochemistry of the Bangombé site.

Numerous isotopic studies on samples from Oklo have been already made to elucidate the phenomenon (e.g., IAEA, 1975, 1978; De Laeter et al., 1980; Loss et al., 1984; Curtis et al., 1989; Janeczek and Ewing, 1996). Variations in the isotopic compositions resulting from the nuclear reactions provide good indicators of the geochemical behaviour of fission products in and around the RZs. Most of these isotopic data have been obtained from RZs 1 to 9, however. As samples from RZs 1 to 9 were taken when they were exposed, some fission products had already migrated in the oxidizing condition of the equatorial climate.

Different data on the behaviour of the fission products can be obtained from the studies on RZs 10, 13, and 16, since they are found in a more reducing environment than that of the RZs 1–9. The relationship between the migration mechanism of fission products and the geochemical conditions in which they are found can thus be studied at Oklo by comparing analyses of RZs found in different conditions of oxidation-reduction. Recent isotopic results obtained from RZ 10 samples show that chemical fractionation between Pu and U (albeit very slight, involving around 1 ppm) has occurred in the SF29 borehole resulting in a local ^{235}U isotopic enrichment of 1.05% (Bros et al., 1993). In addition, it has been shown that part of the fissiogenic alkaline and alkaline earth elements in the SF84 borehole were mobilized during the first stage of reactor functioning (Hidaka et al., 1993a). These facts were deduced from isotopic analyses of RZ 10 and have not been observed in RZs 1–9.

The nuclear parameters can be evaluated from the isotopic compositions of the elements found in the RZs. Because these fission reactors have never been controlled artificially, the functional conditions of the fission reactions are often different from one RZ to another (Naudet, 1991). Differences observed in the nuclear parameters are closely linked to the local geological conditions, such as the U content, the proportion of water acting as moderator of neutrons, and the concentrations of elements which are neutronic absorbers (Loubet and Allegre, 1977; Holliger and Devillers, 1981; Hidaka and Masuda, 1988; Loss et al., 1988; Gauthier-Lafaye et al., 1996). In this paper, we present new findings from three types of RZs and the nuclear parameters deduced from isotopic and elemental analyses.

The geochemical behaviour of the actinides ^{240}Pu and ^{237}Np, produced by neutron capture in the RZs, can be assessed from the nuclear parameters and the measured concentrations of Th and Bi, respectively. Fréjacques et al. (1975) measured the quantities of nucleogenic ^{232}Th and ^{209}Bi in samples from

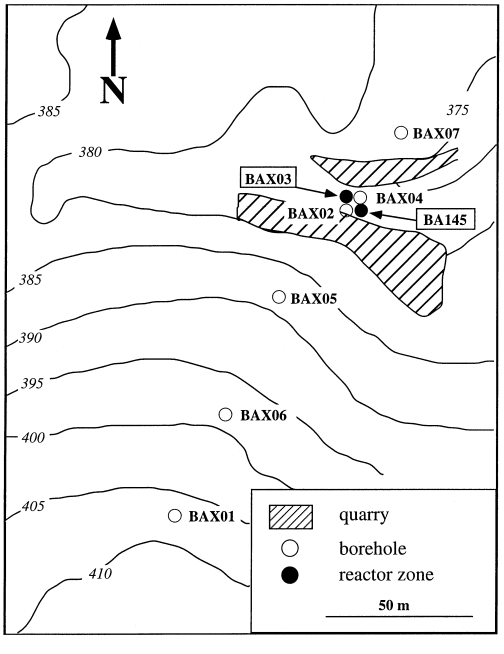

Fig. 2. The location of bore-holes at Bangombé. The RZ is recognized from two bore-holes, BAX3 and BA145.

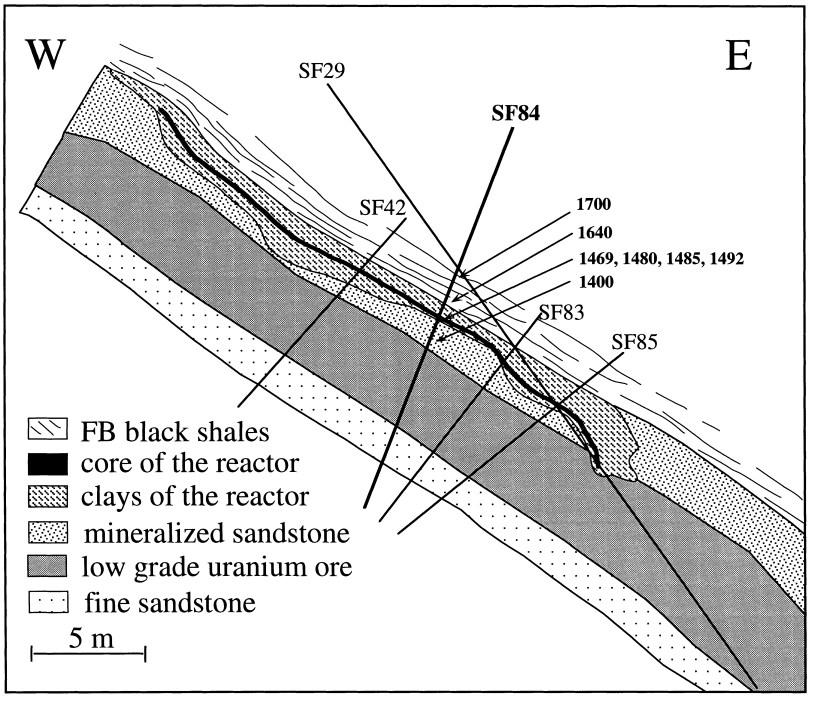

Fig. 3. Cross section of RZ 10 (Gauthier-Lafaye et al., 1996).

borehole SC36 of RZ 2, and demonstrated the retention of ^{240}Pu and ^{237}Np, respectively. We also have tried to compare the measured and calculated abundances of nucleogenic ^{232}Th and ^{209}Bi in RZs 10, 13, and Bangombé, and we discuss the retention of ^{240}Pu and ^{237}Np in these reactors.

2. SAMPLES

Nine samples collected from three types of RZs were used in this study: Seven samples were systematically taken from one of sampling drill-holes, SF84 at RZ 10, one from the center of the reactor core of gallery SD37 at RZ 13, and one from the reactor core of the BA145 borehole at Bangombé.

2.1. SF84 (RZ10, Oklo)

The cross-section of RZ 10 and sampling drill-holes, including SF84, are illustrated by Fig. 3. The nomenclature of the samples follows their real position in cm from the start of the borehole in the gallery. These are the same samples for which the isotopic deviations of alkali and alkaline earth elements have been previously reported (Hidaka et al., 1993a, 1994). SF84 contains a reactor core of approximated 70 cm thickness between 1460 and 1530. Samples 1469, 1480, 1485, and 1492 were from the reactor core, and they consist mainly of uraninite and organic matter. Sample 1400 was from the sandstone (FA) layer below the reactor core, and 1640 and 1700 were from the green pelite (FB) layer above the reactor core. The stratigraphic log of the SF84 drill-hole with sample location is indicated in Fig. 4. The definition of the stratigraphic layers including the Oklo mine, that is the FA to FE formations, has been described in detail by Gauthier-Lafaye and Weber (1989).

2.2. SD37 (RZ13, Oklo)

Significant remobilization of U and Pb have occurred in RZ 13 and are probably linked to the thermal effect of the mag-

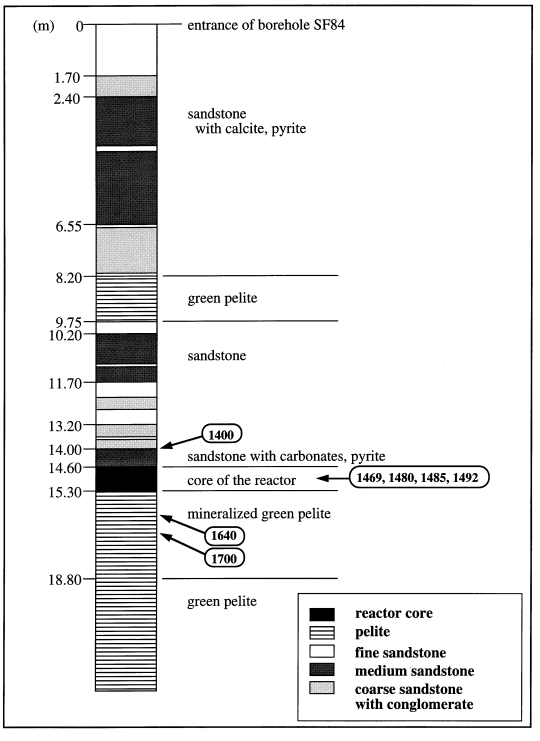

Fig. 4. Stratigraphic description of SF84 drill-hole at RZ 10 (Gauthier-Lafaye et al., 1996).

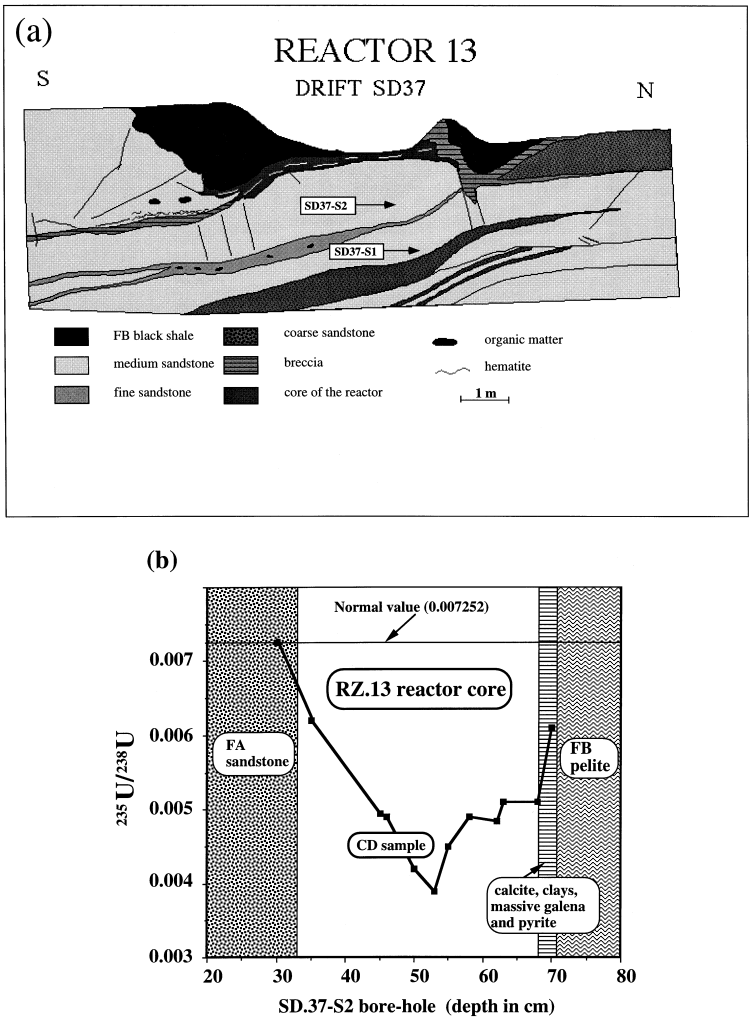

Fig. 5. (a) Cross section of gallery SD37 at RZ 13 (Gauthier-Lafaye, pers. commun.) and (b) distribution profile of ^{235}U depletion in the SD37-S2 borehole.

matic intrusion (Holliger, 1992, 1995; Nagy et al., 1993; Gauthier-Lafaye et al., 1996). Temperatures could have reached 400°C locally in the RZ thus contributing to the elimination of organic material initially present. RZ 13 was found at a height of 6 m between two galleries, SD35 and SD37. The RZ is 30 cm thick, 6 m wide, and 10 m long. Figure 5 illustrates the SD37 gallery at RZ 13 and the depletion profile of ^{235}U in borehole SD37-S2. The sample SD37-S2/CD was taken from a part of high depletion of ^{235}U ($^{235}U/^{238}U = 0.004630$) in this borehole (Holliger, 1993b). Due to the particular conditions, this RZ appears to be different from the other RZs discovered; the results presented hereafter support these observations.

2.3. BA145 (Bangombé)

Bangombé RZ has been found only in boreholes of BAX3 and BA145 (Fig. 2). The RZ is located at 12 m depth. Isotopic study of fissiogenic nuclides of BAX3 was reported by Bros et al. (1994). There are no isotopic data for BA145. Sample BA145.1160 was taken from the reactor core at a depth of 1160 cm in borehole BA145. The reactor core in BA145 is about 10 cm thick.

The characteristics of these samples and their compositions in uranium isotopes are given in Table 1.

3. EXPERIMENTAL METHODS

In order to obtain pure fractions for measurements by mass spectrometry, chemical separation of each element must be done from the sample in solution.

3.1. Whole Rock Analyses with TIMS and ICP-MS

Approximately one gram of each powdered sample was dissolved in 2M HNO_3 without heat. The residue was decomposed by heated HF and $HClO_4$ and was finally dissolved in 2M HNO_3. Such an acid digestion technique is suitable for the preparation of Rb, Sr, Zr, Ag, Ba, REE, and U analyses, but unsuitable for the analyses of Ru, Rh, Pd, and Te. Large amounts of fissiogenic Ru, Rh, Pd, and Te in RZs have been incorporated into the micrometallic aggregates in RZ samples (Holliger, 1992; Hidaka et al., 1994; Gauthier-Lafaye et al., 1996). Because of the difficulty for dissolving metallic aggregates by acids, another aliquot of each powdered sample was attacked by sodium peroxide in

Table 1. List of samples

Zone	Nomenclature	Petrography	U (wt. %)	$^{235}U/^{238}U$*
RZ 10	SF84-1400	FA sandstone	2.99 ± 3	0.007254 ± 15
	SF84-1469	Core of RZ	17.2 ± 2	0.006048 ± 9
	SF84-1480	Core of RZ	7.06 ± 7	0.005069 ± 7
	SF84-1485	Core of RZ	14.9 ± 1	0.005649 ± 12
	SF84-1492	Core of RZ	24.3 ± 3	0.005793 ± 18
	SF84-1640	FB green pelite	0.240 ± 3	0.007248 ± 9
	SF84-1700	FB green pelite	0.0840 ± 8	0.007247 ± 9
RZ 13	SD37-S2/CD	Core of RZ (uraninite)	59.4 ± 6	0.004630 ± 6
Bangombé	BA145-1160	Core of RZ (uraninite)	45.0 ± 4	0.006616 ± 16

* Terrestrial standard value = 0.007252 ± 14.
All standard errors are 2σ means.

a carbon crucible with heat and redissolved with 6M HCl for Ru, Rh, Pd, and Te analyses.

In order to obtain mass spectrometric samples for the measurements with TIMS and ICP-MS, chemical separation of each element from the sample solution was required. Chemical separation procedures were carried out following the conventional methods: Rb and Sr (Faure and Powell, 1972), Zr (Minster and Allegre, 1981; Hidaka et al., 1994), Pd, Ag, and Te (Loss et al., 1983), Ru (Hidaka et al., 1991), Ba (Eugster et al., 1969), REE (Hidaka et al., 1988), and U (Chen and Wasserburg, 1981). Chemically separated fractions by the above procedures were pure, and isobaric interferences from other elements were not detected during the isotopic measurements. The acid reagents used in this study were obtained by double subboiled distillation of super special grade reagents, and water was obtained from millipore (Milli Q). The contamination from reagents and water were negligibly low. Isotopic compositions of each element were determined with TIMS instruments (JEOL JMS-05RB and VG Sector 54) and ICP-MS instrument (VG PlasmaQuad I modified to II plus type).

Mass spectrometric techniques used in this study were previously reported (Hidaka et al., 1992). The correction for instrumental isotopic mass fractionation by ICP-MS has been made using measurements obtained on standard reference materials from Wako Pure Chemical Industries Co., Ltd. (Masuda et al., 1986). The calculated fractionation value for each element is then applied to each unknown elementary isotopic composition in the sample in order to obtain the true isotopic composition. After the determination of isotopic compositions, most of elemental abundances were measured with isotope dilution method by TIMS and ICP-MS. Abundances of monoisotopic elements such as Cs, Pr, Tb, Ho, Tm, Bi, and Th were determined with ICP-MS.

3.2. Thin Section Analyses with SIMS

In situ ruthenium isotopic measurements of metallic inclusions in the RZ samples were performed with a secondary ion mass spectrometer (SIMS), Cameca IMS-3f. Typically, the spot size of O_2^+ primary beam was 10 μm in diameter, and the sputtered area was equivalent in size. Secondary ion beam intensity was in the range of 10^{-12} A for ^{101}Ru isotope in each metallic inclusion. Due to the lack of ruthenium isotope reference standard materials in a matrix such as the metallic inclusion, the instrumental mass discrimination effect on ruthenium isotopic analyses was assumed to be closed to that of Pb in PbS, i.e,. less than 0.3% per amu. The detailed experimental procedures by SIMS were the same as those described by Holliger (1988, 1993b).

4. RESULTS AND DISCUSSION

Depletion of ^{235}U in the samples suggests that fission reactions have undoubtedly occurred in the cores of SF84, SD37, and BA145. On the other hand, wall rock samples from sandstone (SF84-1400) and green pelite layers (1640 and 1700) at SF84 show no depletion of ^{235}U (Table 1). Isotopic compositions of Rb, Sr, Zr, Ru, Pd, Ag, Te, Ba, and REEs in samples are given in Table 2.

The elements of RZ samples have two origins, fissiogenic and nonfissiogenic fractions. Furthermore, the nonfissiogenic fraction contains primordially existing isotopes (pre-reactor elements) which had been incorporated into the ore during its deposition and the natural contaminants from the reactor surroundings after the cessation of reactors (post-reactor elements). Isotopic compositions of post-reactor elements are independent on nuclear reactions, while those of primordial elements vary mainly due to neutron capture reactions in the reactor. The relative abundances between fissiogenic and nonfissiogenic components in the RZ samples can be quantitatively estimated from the isotopic deviations of the elements (Hidaka et al., 1988). The systematic analyses of the isotopic compositions of various elements allow us to characterize the RZs in terms of their nuclear parameters and to discuss the geochemical behavior of fission-produced isotopes.

Through analyses of a series of samples from the SF84 borehole, the variations of isotopic deviations and the differences of the elemental abundances between fissiogenic and nonfissiogenic components were found in each interval of several centimeters along the borehole (see Tables 2 and 3). These data indicate that fission events have occurred heterogeneously, at least on the scale of several centimeters and/or the elements including fission products might have been redistributed within the reactor.

4.1. Isotopic Characterization of Natural Fission Reactors

The estimation of nuclear parameters of reactors is required to elucidate the fission mechanism in the natural fission reactors. Some of REE isotopes such as ^{143}Nd, ^{149}Sm, ^{155}Gd, and ^{176}Lu sensitively interact with fission-released neutrons because of their large neutron capture cross-sections. Nuclear parameters of analyzed samples can be quantitatively calculated by using isotopic deviations of such nuclides.

4.1.1. Neutron fluence (τ), spectrum index (r), and restitution factor of ^{235}U (C)

Neutron fluences (n/cm^2), the spectrum index (r) of fission-released neutrons, and the restitution factor of ^{235}U from ^{239}Pu (C) are calculated from the combination of the $^{235}U/^{238}U$ and $^{144}Nd/^{143}Nd$ ratios (Ruffenach et al., 1976; Holliger, 1993a).

The fundamental concept is as follows. The production rate

Table 2. Isotopic data of Oklo and Bangombé reactor samples (expression by atom % or isotopic ratio).

	STD	1400	1469	1480	1485	1492	1640	1700	SD.37	BA145.1160
Rb										
85	72.15 ± 4	71.92 ± 7	66.92 ± 9	60.51 ± 6	61.64 ± 7	70.23 ± 6	72.15 ± 11	72.16 ± 10	72.02 ± 12	72.12 ± 1
87	27.85 ± 1	28.08 ± 2	33.08 ± 5	39.49 ± 4	38.36 ± 4	29.77 ± 3	27.85 ± 4	27.84 ± 4	27.98 ± 4	27.88 ± 1
Sr										
87/86	0.71030 ± 30	0.71961 ± 47	0.72985 ± 72	0.71488 ± 71	0.72752 ± 78	0.73746 ± 95	n.a.	n.a.	0.7509 ± 44	n.a.
88/86	8.3729 ± 37	8.3712 ± 41	8.8084 ± 99	8.4713 ± 74	8.9120 ± 86	9.6160 ± 92	8.3735 ± 78	8.3755 ± 81	8.3786 ± 21	8.3759 ± 33
Zr*										
90	51.44 ± 5	51.89 ± 36	47.09 ± 32	51.34 ± 35	48.65 ± 34	49.71 ± 34	51.32 ± 35	51.85 ± 37	27.68 ± 17	
91	11.21 ± 1	11.16 ± 7	12.34 ± 8	11.26 ± 7	12.02 ± 7	11.66 ± 8	11.37 ± 8	11.18 ± 8	16.43 ± 8	
92	17.15 ± 2	17.10 ± 11	17.57 ± 11	17.17 ± 11	17.39 ± 10	17.25 ± 12	17.19 ± 11	16.88 ± 11	18.77 ± 8	
94	17.39 ± 2	17.10 ± 11	17.83 ± 11	17.33 ± 10	17.69 ± 10	17.46 ± 10	17.29 ± 10	17.13 ± 10	21.02 ± 11	
96	2.798 ± 3	2.735 ± 11	5.170 ± 25	2.904 ± 11	4.243 ± 12	3.908 ± 12	2.831 ± 11	2.952 ± 11	16.10 ± 8	
Ru*										
96	5.553 ± 15		<0.01	<0.01	<0.01	<0.01			<0.01	<0.01
98	1.873 ± 19		<0.01	<0.01	<0.01	<0.01			<0.01	<0.01
99	12.45 ± 15		33.99 ± 25	33.90 ± 28	32.39 ± 15	33.29 ± 23			33.55 ± 43	33.02 ± 18
100	12.43 ± 4		0.613 ± 13	0.542 ± 9	0.464 ± 9	0.477 ± 16			0.960 ± 6	0.242 ± 29
101	17.09 ± 5		28.63 ± 4	28.85 ± 9	29.74 ± 20	29.36 ± 11			27.36 ± 8	29.57 ± 16
102	31.94 ± 15		24.49 ± 4	24.55 ± 25	25.18 ± 17	24.86 ± 9			24.27 ± 7	25.02 ± 6
104	18.66 ± 10		12.28 ± 7	12.16 ± 2	12.16 ± 10	12.01 ± 3			13.86 ± 4	12.15 ± 2
Pd*										
106/105	1.2069 ± 35		0.5258 ± 20	0.5729 ± 175		0.5308 ± 116			0.6623 ± 110	
108/105	1.1617 ± 40		0.1315 ± 27	0.1812 ± 107		0.1302 ± 14			0.2220 ± 22	
110/105	0.5184 ± 27		0.0528 ± 22	0.0765 ± 19		0.0512 ± 12			0.0747 ± 8	
Ag										
107	52.03 ± 2		49.21 ± 17	56.65 ± 31		60.73 ± 63			60.57 ± 32	
109	47.97 ± 2		50.79 ± 18	43.35 ± 23		39.27 ± 40			39.43 ± 21	
Te										
120/128	0.03057 ± 12	n.a.	<0.01	<0.01		<0.01			<0.01	
122/128	0.08195 ± 8	n.a.	<0.01	<0.01		<0.01			<0.01	
123/128	0.02873 ± 12	n.a.	<0.01	<0.01		<0.01			<0.01	
124/128	0.1507 ± 1	n.a.	<0.01	<0.01		<0.01			<0.01	
125/128	0.2232 ± 2	0.2447 ± 93	0.1179 ± 7	0.1196 ± 12		0.1043 ± 11			0.1157 ± 4	
126/128	0.5936 ± 4	0.5474 ± 19	0.1369 ± 4	0.1762 ± 2		0.1334 ± 4			0.1154 ± 2	
130/128	1.0688 ± 7	1.300 ± 13	5.038 ± 9	4.993 ± 18		5.173 ± 13			4.514 ± 5	
Ba										
134/136	0.30918 ± 32	0.31036 ± 51	0.31483 ± 57	0.31028 ± 70	0.31326 ± 62	0.31365 ± 80	0.30902 ± 61	0.30882 ± 51	0.31034 ± 59	0.30786 ± 12
135/136	0.83994 ± 81	0.83998 ± 108	0.90775 ± 159	0.84238 ± 144	0.98199 ± 152	1.04218 ± 192	0.83970 ± 141	0.83997 ± 157	0.84034 ± 157	0.83940 ± 42
137/136	1.4283 ± 10	1.4299 ± 20	1.5228 ± 32	1.4303 ± 34	1.5596 ± 36	1.6182 ± 35	1.4301 ± 18	1.4306 ± 21	1.4315 ± 19	1.4289 ± 7
138/136	9.1298 ± 80	9.1941 ± 160	9.5773 ± 178	9.1290 ± 158	9.1986 ± 179	9.4483 ± 123	9.1254 ± 116	9.1288 ± 105	9.1305 ± 137	9.1232 ± 44
La										
138	0.09003 ± 8		0.01290 ± 2	0.01285 ± 3			0.09007 ± 9	0.08899 ± 9		
139	99.910 ± 89		99.987 ± 155	99.987 ± 233			99.909 ± 101	99.911 ± 101		
Ce										
136	0.1870 ± 4	0.1873 ± 17	0.03029 ± 20	0.03230 ± 28	0.05368 ± 55	0.03175 ± 69	0.1862 ± 7	0.1874 ± 13	0.02415 ± 9	0.1163 ± 9
138	0.2550 ± 4	0.2462 ± 26	0.03734 ± 25	0.04168 ± 39	0.06422 ± 79	0.05686 ± 81	0.2469 ± 21	0.2551 ± 13	0.03682 ± 14	0.1326 ± 10
140	88.30 ± 10	87.83 ± 10	56.06 ± 7	57.96 ± 9	61.28±14	58.24 ± 14	88.34 ± 18	88.30 ± 12	55.28 ± 8	64.38 ± 10
142	11.26 ± 2	11.74 ± 1	43.87 ± 5	41.97 ± 6	38.61 ± 9	41.67 ± 10	11.23 ± 2	11.26 ± 2	44.60 ± 7	35.35 ± 5
Nd										
142	27.19 ± 3	26.67 ± 6	1.033 ± 4	1.666 ± 6	2.166 ± 9	1.436 ± 7	28.45 ± 10	27.52 ± 3	1.006 ± 1	5.453 ± 23
143	12.18 ± 2	12.47 ± 3	25.86 ± 4	24.35 ± 4	24.86 ± 4	25.54 ± 5	11.95 ± 4	12.19 ± 1	24.83 ± 1	24.42 ± 5
144	23.80 ± 2	24.00 ± 5	28.55 ± 5	29.68 ± 8	28.82 ± 6	28.76 ± 11	23.33 ± 8	23.68 ± 2	29.68 ± 1	27.09 ± 6
145	8.290 ± 10	8.527 ± 17	18.25 ± 3	17.90 ± 3	17.81 ± 4	18.11 ± 7	8.191 ± 27	8.262 ± 8	17.83 ± 1	16.65 ± 4
146	17.17 ± 3	17.08 ± 4	14.90 ± 2	15.04 ± 4	14.97 ± 3	15.08 ± 3	17.03 ± 6	17.10 ± 2	15.04 ± 1	15.12 ± 3
148	5.744 ± 4	5.782 ± 1	8.040 ± 12	8.006 ± 20	7.931 ± 15	7.861 ± 43	5.664 ± 16	5.712 ± 7	8.107 ± 2	7.611 ± 13
150	5.624 ± 4	5.473 ± 1	3.364 ± 5	3.364 ± 7	3.440 ± 7	3.216 ± 19	5.388 ± 17	5.540 ± 6	3.514 ± 1	3.654 ± 11

of ^{143}Nd by fission and neutron capture reaction is expressed as follows:

$$dN/dt = N_{235}\cdot\rho\cdot\sigma_{f235}\cdot\Phi - N\cdot\sigma_c\cdot\Phi, \quad (1)$$

where ρ is a fission yield of ^{143}Nd, σ_{f235} is a fission cross-section of ^{235}U; Φ is a neutron flux, namely the time integration of Φ indicates neutron fluence $\tau(\Sigma\Phi = \tau)$; N and N_{235} are the number of ^{143}Nd and ^{235}U atoms at the time of criticality, respectively; σ_c is the cross-section for ^{143}Nd(n, γ)^{144}Nd and practically can be written as $\sigma_c = 325 + 140r$; r is a spectrum index for the neutrons.

In addition, the number of ^{235}U atoms is also a function of time.

$$dN_{235}/dt = -N_{235}\cdot\sigma_{235}\cdot(1 - C)\cdot\Phi, \quad (2)$$

where C is a restitution factor of ^{235}U reproduced as α decay products of ^{239}Pu after the neutron capture of ^{238}U.

Table 4 shows the results of these nuclear parameters obtained from the combination of Eqns. 1 and 2. The neutron fluence in the SF84 varies from 5.3×10^{20} to 8.0×10^{20} (n/cm^2). The nuclear parameters (τ, r, C), the degrees of ^{235}U depletion (^{235}U/^{238}U), and U content (wt%) along the location of SF84 core are plotted in Fig. 6. There are differences beyond the calculated errors in these parameters between the center (SF84-1480, 1485, and 1492) and the edges (SF84-1469 and 1521) even in the same RZ. The center of reactor core (1480) indi-

Table 2. Continued.

	STD	1400	1469	1480	1485	1492	1640	1700	SD.37	BA145.1160
Sm										
144	3.127 ± 9	3.194 ± 14	0.1052 ± 6	0.2401 ± 8	0.2073 ± 13	0.1619 ± 11	3.151 ± 8	3.138 ± 5	0.06909 ± 18	0.5342 ± 23
147	15.11 ± 2	15.94 ± 5	55.34 ± 6	53.23 ± 7	54.03 ± 9	54.81 ± 13	15.29 ± 3	15.22 ± 2	52.74 ± 2	50.82 ± 16
148	11.30 ± 2	11.35 ± 3	2.796 ± 3	3.468 ± 8	3.079 ± 8	2.890 ± 8	11.35 ± 3	11.35 ± 2	4.694 ± 2	3.114 ± 6
149	13.86 ± 2	5.800 ± 4	0.5544 ± 32	0.2821 ± 10	0.4466 ± 20	0.4296 ± 17	13.89 ± 4	13.91 ± 2	0.3088 ± 4	2.199 ± 7
150	7.392 ± 14	15.61 ± 6	26.60 ± 2	25.90 ± 7	26.30 ± 5	26.33 ± 5	7.495 ± 22	7.411 ± 11	26.38 ± 2	24.28 ± 7
152	26.65 ± 3	26.31 ± 8	11.68 ± 1	13.07 ± 4	12.42 ± 2	12.15 ± 2	26.59 ± 7	26.56 ± 4	12.53 ± 1	13.49 ± 4
154	22.57 ± 3	21.80 ± 6	2.934 ± 5	3.806 ± 8	3.520 ± 6	3.222 ± 7	22.24 ± 6	22.42 ± 3	3.277 ± 3	5.562 ± 18
Eu										
151	47.88 ± 6	45.50 ± 13	31.61 ± 3	23.97 ± 6	28.17 ± 4	28.31 ± 6	47.56 ± 15	47.85 ± 7	22.06 ± 1	45.69 ± 8
153	52.12 ± 7	54.50 ± 16	68.39 ± 6	76.03 ± 17	71.83 ± 11	71.69 ± 15	52.44 ± 16	52.15 ± 8	77.94 ± 6	54.31 ± 9
Gd										
152	0.2011 ± 2	0.3674 ± 22	26.59 ± 7	22.74 ± 9	21.21 ± 9	26.46 ± 10	0.2285 ± 18	0.2373 ± 20	28.65 ± 11	10.42 ± 2
154	2.176 ± 18	2.255 ± 7	7.970 ± 20	9.773 ± 37	7.746 ± 31	8.566 ± 32	2.231 ± 9	2.227 ± 4	16.79 ± 6	3.614 ± 8
155	14.78 ± 3	10.37 ± 3	0.5006 ± 21	0.4608 ± 39	0.6065 ± 42	0.3899 ± 15	14.78 ± 3	14.84 ± 3	0.5915 ± 31	5.816 ± 13
156	20.46 ± 6	25.04 ± 7	30.03 ± 6	29.46 ± 9	30.79 ± 12	29.90 ± 9	20.55 ± 6	20.59 ± 4	30.37 ± 13	28.41 ± 6
157	15.67 ± 6	4.056 ± 12	0.04176 ± 86	0.2641 ± 25	0.1929 ± 13	0.05045 ± 77	15.70 ± 4	15.68 ± 3	0.1881 ± 8	5.346 ± 16
158	24.79 ± 9	36.12 ± 13	23.66 ± 5	25.07 ± 9	26.52 ± 13	23.68 ± 6	24.84 ± 6	24.80 ± 4	17.31 ± 4	28.75 ± 6
160	21.92 ± 6	21.79 ± 8	11.21 ± 3	12.24 ± 5	12.93 ± 5	10.95 ± 4	21.67 ± 5	21.63 ± 4	6.103 ± 22	17.65 ± 3
Dy										
156	0.0600 ± 7	<0.1	n.a.		<0.1	n.a.	<0.1	<0.1		
158	0.0969 ± 6	0.1690 ± 14	n.a.		0.2388 ± 10	n.a.	0.1065 ± 4	<0.1		
160	2.414 ± 9	2.418 ± 5	4.966 ± 23		3.719 ± 25	3.782 ± 30	2.297 ± 14	2.390 ± 5		
161	19.05 ± 4	19.08 ± 3	18.32 ± 7		17.45 ± 3	17.06 ± 8	19.25 ± 6	18.94 ± 2		
162	25.66 ± 4	25.78 ± 4	30.41 ± 12		30.96 ± 6	31.74 ± 14	25.56 ± 12	25.50 ± 3		
163	24.71 ± 4	25.02 ± 4	32.62 ± 14		34.48 ± 8	36.28 ± 17	24.48 ± 8	24.86 ± 4		
164	28.00 ± 11	27.53 ± 4	13.69 ± 4		13.16 ± 3	11.14 ± 7	28.30 ± 9	28.03 ± 4		
Er										
162	0.1450 ± 27	0.1860 ± 50		0.1528 ± 10	0.1347 ± 8	0.1204 ± 11	n.a.	0.1493 ± 31		
164	1.602 ± 14	1.662 ± 10		1.561 ± 10	1.533 ± 13	1.5672 ± 62	1.606 ± 24	1.611 ± 7		
166	33.37 ± 2	33.40 ± 7		34.89 ± 10	34.93 ± 10	35.14 ± 8	33.48 ± 14	33.98 ± 6		
167	22.87 ± 4	22.70 ± 4		6.942 ± 19	8.729 ± 24	8.308 ± 18	22.76 ± 9	22.82 ± 4		
168	26.99 ± 4	27.27 ± 5		42.16 ± 12	39.78 ± 11	40.58 ± 7	27.29 ± 11	26.70 ± 7		
170	15.00 ± 3	14.79 ± 5		14.30 ± 6	14.12 ± 6	14.29 ± 3	14.87 ± 9	14.74 ± 4		
Yb										
168	0.1364 ± 4	0.1212 ± 13	<0.1	<0.1	<0.1	<0.1	n.a.	n.a.	<0.1	
170	3.072 ± 3	3.063 ± 16	5.659 ± 27	6.245 ± 23	5.550 ± 5	5.697 ± 19	2.917 ± 20	3.109 ± 12	7.361 ± 23	
171	14.29 ± 2	14.39 ± 5	13.65 ± 8	13.56 ± 4	13.67 ± 1	13.58 ± 5	14.26 ± 6	14.26 ± 7	13.21 ± 7	
172	21.79 ± 2	21.73 ± 7	22.14 ± 13	22.21 ± 7	21.89 ± 2	22.17 ± 8	21.78 ± 9	22.02 ± 11	22.28 ± 12	
173	16.14 ± 3	16.12 ± 6	15.26 ± 8	14.77 ± 6	15.01 ± 3	15.10 ± 6	15.62 ± 6	16.30 ± 6	14.76 ± 6	
174	31.78 ± 2	31.79 ± 14	30.81 ± 16	30.52 ± 11	31.24 ± 4	31.00 ± 12	32.25 ± 14	31.46 ± 13	30.03 ± 8	
176	12.79 ± 2	12.78 ± 4	12.50 ± 7	12.71 ± 3	12.64 ± 1	12.45 ± 5	13.18 ± 6	12.86 ± 5	12.35 ± 4	
Lu										
175	97.348 ± 30	97.370 ± 22	99.695 ± 98	99.479 ± 190	99.866 ± 60	99.377 ± 112	97.366 ± 30	97.352 ± 26		99.446 ± 105
176	2.652 ± 6	2.630 ± 6	0.305 ± 3	0.521 ± 10	0.134 ± 1	0.623 ± 7	2.634 ± 8	2.648 ± 7		0.554 ± 6

* Measured by ICP-MS. Others are by TIMS.
n.a. = not analysed.
All standard errors are 2σ means.

cates the highest neutron fluence in SF84 core, while the edges of the reactor (1469 and 1521) have a lower neutron fluence. On the other hand, the patterns of the restitution factors (C) and of spectrum index (r) in SF84 have an inverse trend to that of neutron fluence. The differences in these patterns suggest the heterogeneity of neutron flux energy in the RZ. The conditions for some fission-released neutrons to induce further fission in the vicinity of RZ were more effective than those around the RZ boundary. The conditions for fission are influenced by the existence of neutron absorber elements and the water content in a sample. Fission-released neutrons would be thermalized around sample 1480, while neutrons might not be well thermalized near the boundaries. Though the reactor core of SF84 is at most 70 cm thick, the conditions of fission vary in each on the scale of several centimeters.

Isotopic abundances of ^{155}Gd and ^{157}Gd in all of the reactor core samples decrease nearly up to zero, because neutron capture reactions for ^{155}Gd and ^{157}Gd had intensively proceeded nearly to completion and turned to ^{156}Gd and ^{158}Gd, respectively. Therefore, the estimation of neutron fluence from the gadolinium isotopic compositions (Hidaka and Masuda, 1988) should be a useful method to determine the neutron fluence in nature (Eugster et al., 1970; Lingenfelter et al., 1972; Maas and McCulloch, 1990), but is not necessarily applicable to the RZ samples with high neutron fluences greater than 10^{20} neutrons/cm^2.

Some REE such as Ce, Nd, Sm, Eu, and Gd in the sandstones (SF84-1400) located 60 cm below the SF84 reactor core have slight but significant isotopic anomalies in spite of showing no depletion of ^{235}U (^{235}U/^{238}U = 0.007254 ± 15). Menet et al.(1992) reported isotopic evidence for migration of fissiogenic Nd from a D73 core (RZ 10) along carbonate fissures to sandstone. For SF84-1400, the isotopic deviations of the REEs were probably the result of migration of fission products into the sandstone layer. As described later, the isotopic composition of Te in SF84-1400 shows a slight contamination of fission products, although Te is considered to be the most retentive element as compared with U (Curtis et al., 1989). Assuming

Table 3. Elemental concentrations of Oklo and Bangombé reactor samples (ppm).

	1400	1469	1480	1485	1492	1640	1700	SD.37	BA145.1160
Rb	0.0900 (2)	6.74 (5)	1.06 (2)	1.40 (2)	8.94 (14)	1.84 (3)			
Sr	247 (1)	89.1 (5)	162 (2)	114 (1)	112 (1)	14.3 (2)			
Zr	2840 (23)	1150 (34)	11600 (92)	4540 (46)	1780 (33)	108 (2)	600 (8)	6360 (67)	
Ru		200 (4)	71.6 (12)	195 (4)	306 (3)			830 (8)	224 (4)
Rh		38.0 (9)	14.0 (3)		50.5 (9)			203 (4)	
Pd		26.9 (9)	11.1 (3)		37.2 (7)			157 (3)	
Te		34.5 (3)	12.4 (2)		48.8 (5)			120 (1)	
Cs	0.321 (5)	12.5 (3)	6.02 (7)	14.8 (4)	30.4 (4)	11.1 (3)			
Ba	247 (2)	453 (4)	290 (2)	322 (3)	574 (4)	822 (4)			
La	199 (2)	99.6 (8)	70.0 (5)	119 (1)	210 (2)	1.82 (1)	13.5 (1)	203 (2)	106 (2)
Ce	225 (2)	231 (1)	109 (1)	313 (3)	453 (2)	10.1 (1)	65.1 (5)	712 (6)	386 (4)
Pr	38.8 (6)	95.8 (9)	42.7 (6)	110 (3)	170 (2)	0.533 (5)	3.60 (2)	411 (3)	144 (4)
Nd	224 (2)	357 (2)	144 (1)	382 (1)	575 (4)	1.95 (2)	14.9 (1)	1540 (11)	523 (4)
Sm	38.9 (3)	67.9 (5)	23.8 (1)	67.6 (4)	112 (1)	0.431 (3)	3.32 (3)	381 (3)	110 (1)
Eu	2.38 (1)	5.96 (2)	3.19 (2)	6.53 (2)	9.63 (9)	0.121 (1)	0.932 (8)	32.5 (2)	19.5 (2)
Gd	42.8 (3)	10.8 (2)	3.87 (4)	15.3 (3)	18.9 (2)	0.317 (4)	2.78 (4)	47.5 (6)	22.0 (3)
Tb	3.87 (5)	1.41 (3)	0.565 (7)	1.51 (1)	1.98 (3)	0.0587 (9)	0.369 (7)	4.16 (5)	1.96 (3)
Dy	15.8 (2)	6.04 (3)	2.49 (2)	5.63 (3)	9.32 (8)	0.321 (4)	1.73 (2)	2.09 (2)	4.36 (4)
Ho	2.78 (4)	1.71 (5)	1.19 (3)	1.97 (3)	2.52 (5)	0.0642 (7)	0.320 (3)	3.56 (4)	1.78 (5)
Er	5.69 (4)	3.71 (2)	3.28 (5)	4.28 (4)	5.83 (4)	0.128 (2)	0.665 (7)	6.00 (6)	4.01 (4)
Tm	0.672 (8)	0.327 (6)	0.285 (5)	0.442 (8)	0.602 (12)	0.0188 (7)	0.0776 (9)	0.261 (3)	0.316 (5)
Yb	3.90 (3)	1.84 (1)	1.67 (4)	2.43 (1)	3.96 (3)	0.0916 (9)	0.567 (7)	1.69 (2)	1.90 (2)
Lu	0.643 (3)	0.934 (9)	0.876 (11)	1.19 (2)	1.71 (3)	0.0228 (4)	0.102 (4)	0.262 (4)	0.336 (5)
Bi	0.371 (15)	21.7 (7)	6.55 (14)	4.50 (9)	23.6 (6)	0.00686 (12)	0.113 (5)	463 (5)	12.0 (5)
Th	328 (10)	805 (12)	168 (4)	253 (5)	918 (9)	0.358 (7)	2.04 (4)	3588 (37)	607 (9)

Number in parentheses are standard deviations of the last digits indicated.

that the isotopic anomalies of Ce and Nd were caused by mixing of fissiogenic and nonfissiogenic components, the contribution rates of fissiogenic Ce and Nd to the total are calculated as 1.3% and 1.6%, respectively. But the isotopic anomalies observed in Sm and Gd cannot be explained by the mixing of fissiogenic and non-fissiogenic components. Isotopic compositions of Sm and Gd in SF84-1400 were possibly created by the neutron capture reactions, rather than migration of fission products. There is some evidence of possible nuclear reactions which started in the sandstone but could not maintain criticality. As shown in Table 2, the ^{149}Sm(n, γ)^{150}Sm, ^{155}Gd(n, γ)^{156}Gd and ^{157}Gd(n, γ)^{158}Gd reactions are observed in samarium and gadolinium isotopic compositions of SF84-1400. The neutron fluence calculated from these isotopic anomalies is 6.2×10^{18} n/cm^2.

The C value of SD37 is much lower than those of other RZ samples, while the spectrum index (r) of SD37 is highest. This suggests that the fission-released neutrons in the vicinity of SD37 were not well thermalized, and ^{238}U preferred fission reaction instead of neutron capture. This interpretation is consistent with the data obtained from the evaluated fission contribution rates of ^{235}U, ^{238}U, and ^{239}Pu (see next paragraph). BA145 seems to be a similar fission reactor to SF84, although its neutron fluence is slightly lower (3.1×10^{20} n/cm^2) than those of SF84 (5.3×10^{20} to 8.0×10^{20} n/cm^2).

4.1.2. Inventory of fission event (α, β, 1-α-β)

The fission inventory of natural fission reactors can be mainly classified into three types; thermal neutron-induced

Table 4. Evaluated values of nuclear parameters for reactor core samples of SF84, SD37, and BA145.

Sample	SF84-1469	SF84-1480	SF84-1485	SF84-1492	SD.37	BA145.1160
RZ	10	10	10	10	13	Bangombé
Neutron fluence (τ: $\times 10^{21} n/cm^2$)	0.525 ± 7	0.798 ± 9	0.622 ± 15	0.564 ± 8	0.780 ± 3	0.308 ± 12
Restitution factor of ^{235}U (C)	0.460 ± 8	0.304 ± 8	0.376 ± 14	0.382 ± 12	0.111 ± 4	0.484 ± 19
Spectrum index (r)	0.181 ± 4	0.111 ± 2	0.140 ± 3	0.155 ± 9	0.241 ± 7	0.196 ± 4
Duration time (Δt: $\times 10^5$ yr)	1.56 ± 1	1.43 ± 1	1.56 ± 2	1.98 ± 1	0.242 ± 1	1.10 ± 1
Average temperature (°C)	>1000	380	>1000	>1000		>1000
Fission contribution						
^{235}U (1-α-β)	0.889 ± 5	0.906 ± 3	0.924 ± 9	0.924 ± 4	0.749 ± 3	0.923 ± 5
^{238}U (α)	0.074 ± 1	0.051 ± 1	0.038 ± 1	0.049 ± 1	0.179 ± 2	0.042 ± 1
^{239}Pu (β)	0.037 ± 1	0.043 ± 1	0.038 ± 1	0.027 ± 1	0.072 ± 1	0.035 ± 1

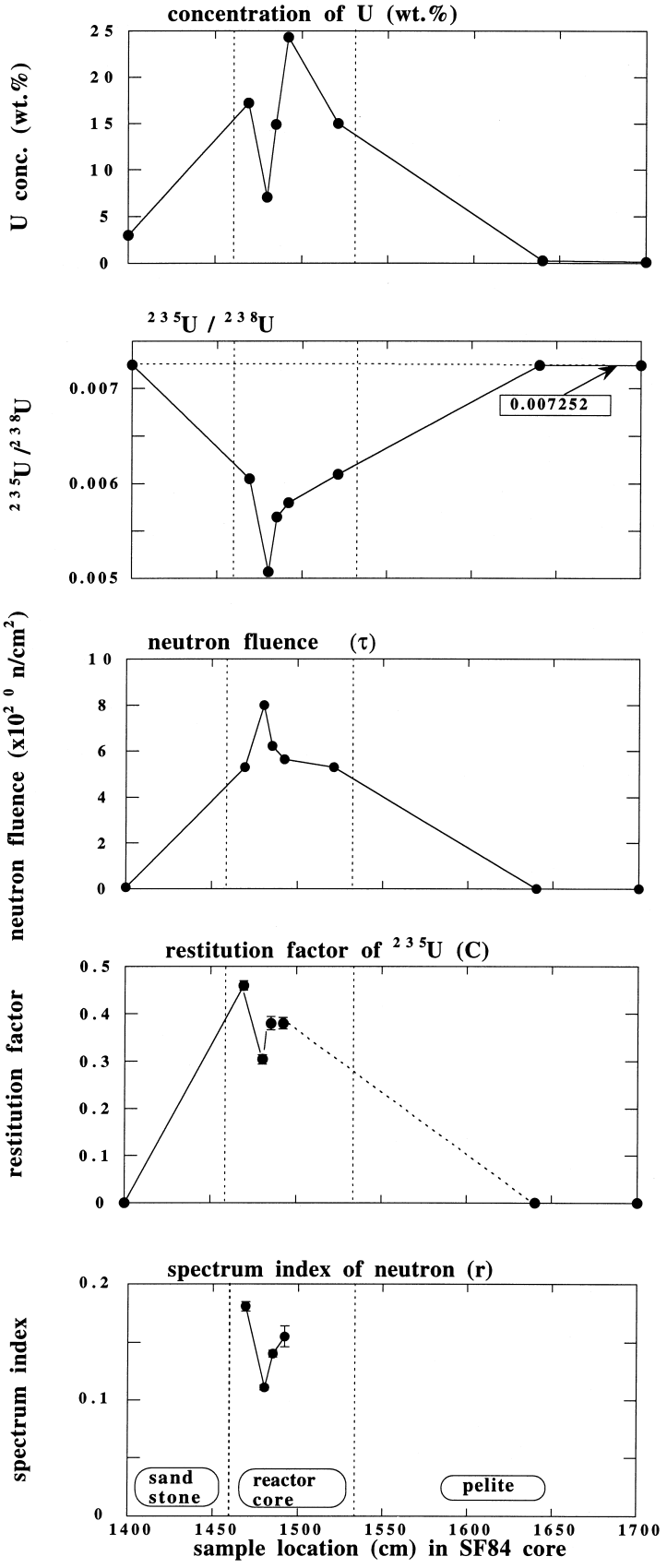

Fig. 6. Variations of uranium concentration (wt%), depletion of ^{235}U ($^{235}U/^{238}U$ ratio), the restitution factor of ^{235}U (C), neutron fluence (t), and neutron spectrum index (r) in the SF84 core at RZ 10. Only the data of SF84-1521 were obtained by SIMS analysis.

fission of ^{235}U, fast neutron induced fission of ^{238}U, and thermal neutron induced fission of ^{239}Pu. Fission contributions of these three fissile nuclides can be calculated from the isotopic ratios of Ru, Pd, Nd, Sm, and/or Gd (Ruffenach et al., 1976), because the fission yields of these elements are remarkably variable in the species of fissile nuclides. Table 4 shows the fission inventory of the RZs SF84, SD37, and BA145 evaluated from ruthenium isotopic ratios $^{102}Ru/^{101}Ru$ and $^{104}Ru/^{101}Ru$. The values of 1-α-β,α, β indicate the contribution rates of ^{235}U, ^{238}U, and ^{239}Pu to the total, respectively. A low α value suggests a high degree of neutron thermalization since the amount of ^{238}U fission depends primarily upon the fast neutron flux in the reactor. In other words, the more the neutrons in a system are thermalized to the advantage of fission for ^{235}U (1-α-β) and ^{239}Pu (β), the lower the α value is in the system. Although SF84 samples were collected from the same borehole, they were located at several centimeter intervals, and slight differences in the fission events are found from the α values.

From the ruthenium isotopic composition, it is evident that fissions in SD37-S2/CD were unusual. The a value of SD37-S2/CD is 0.179 which is much higher than those of the SF84 and BA145 samples. The SD37 sample is quite different from SF84 as a fission reactor. The restitution factor, C, of SD37 is lower than those of the other reactor core samples. According to the critical duration of the reactions (discussed in a following section), the mean neutron flux in SD37 was at least ten times higher than in the other RZs.

4.1.3. Average temperature of neutrons (°C)

^{176}Lu is very sensitive to neutron energy, because its neutron capture cross-section varies largely with neutron energy. Therefore, the $^{176}Lu/^{175}Lu$ isotopic ratio in the RZ samples can be used to evaluate the average equilibrium temperature of the neutrons at the time of criticality (Holliger and Devillers, 1981). However, the isotopic data of Lu do not necessarily provide correct information on the temperature in a system. Holliger and Devillers (1981) evaluated the reactor temperatures of seven samples collected from RZs 2, 3, and 5. Calculated temperatures of six samples varied from 220°C to 360°C, but one sample showed a high temperature greater than 1000°C. In this study, the Lu isotopic composition of SF84-1480 provided 380°C as an average temperature, but other-samples indicated greater than 1000°C. Holliger and Devillers (1981) suggested that heavy rare earth elements could have become enriched in the sample during criticality thus leading to the high calculated temperature. As shown in Table 3, there is little difference in the Lu abundances in the samples in this study. Compared with the relative retentivity of REEs in the RZ10, there is no remarkable difference among REEs. The reliability of the estimated values at high temperature is questionable because of the difficulty of precise measurement of the cross-section of ^{176}Lu. The temperature dependence of the neutron capture cross-section for ^{176}Lu should be investigated in further detail, especially in order to improve the estimated temperatures in the RZs.

4.1.4. Duration of reactor operation (Δt)

Duration of natural reactor operation can be evaluated from the following equation (Hagemann et al., 1975; Ruffenach et al., 1976):

$$\Delta t = \sigma_{f239}\cdot\sigma_{235}\cdot(1-\alpha-\beta)\cdot C\cdot\tau/(\sigma_{f235}\cdot\beta\cdot\lambda_{239}$$

Table 4 gives the calculated Δt values for six RZ samples. Four samples from SF84 show little variation of Δt, 1.43 x 10^5 to 1.98 x 10^5 a. As compared with a variation of Δt (0.64 x 10^5 a to 5.56 x 10^5 a) in RZ 9 calculated by Loss et al. (1988), the periods of criticality in the SF84 core roughly agree with each other. Considering uncertainties of the estimated Δt value derived from the errors of cross-sections, decay constants, and nuclear parameters (α, β, C, τ), Δt in BA145 is similar to those in SF84. On the other hand, SD37 has a shorter duration than those of SF84. The fission condition at SD37 is largely different from other RZs.

All of the nuclear parameters are based on the isotopic abundances of U and fission products. If these elements have been removed from the point of reaction or large differentiation has occurred between U and fission products after cessation of the reactor operation, the view of estimates of nuclear parameters will have no meaning. Thus, from the point of view of both estimate of nuclear parameters and the migration of radionuclides in the environment, it is essential to investigate the behavior of fissiogenic isotopes in the reactor.

4.2. Fission Product Yields

In order to evaluate the retentivities of fissiogenic nuclides, the fission product yield curves can be used effectively (Fréjacques et al., 1975; Roth, 1977; Hagemann and Roth, 1978). In our previous study (Hidaka et al., 1992), we tried to determine fission product yield curves of Oklo samples and provided information on the geochemical behavior of fissiogenic nuclides. In the same manner, the relative fission product yield curves of RZ samples are given from the isotopic abundances of fissiogenic nuclides. Figure 7 shows the relative fission product yield curves of six RZ samples (SF84-1469, 1480, 1485, 1492, SD37-S2/CD, and BA145-1160). The open circles in each figure indicate the expected fission yields after consideration of the fission contribution rates of ^{235}U, ^{238}U, and ^{239}Pu in each sample. The degree of deviation between observed yields (closed circles) and expected yields (open circles) is a measure of the stability of fissiogenic nuclides in a sample. Comparing previous Oklo studies of fissiogenic nuclide migration in RZs 1-9 (Loubet and Allegre, 1977; DeLaeter et al., 1980; Holliger and Devillers, 1981; Loss et al., 1984; Curtis et al., 1989; Hidaka et al., 1992) with this study of RZs10, 13, and BA145, there are some similarities and differences which are summarized in the following sections.

4.2.1. Rare earth elements

All fissiogenic REEs have been well retained in U matrices of the RZs, because the crystallochemical properties of REEs are similar to those of U (Burns et al., 1997). According to previous isotopic studies on RZ9, the possibility of partial migration of fissiogenic La and Ce from other REEs was

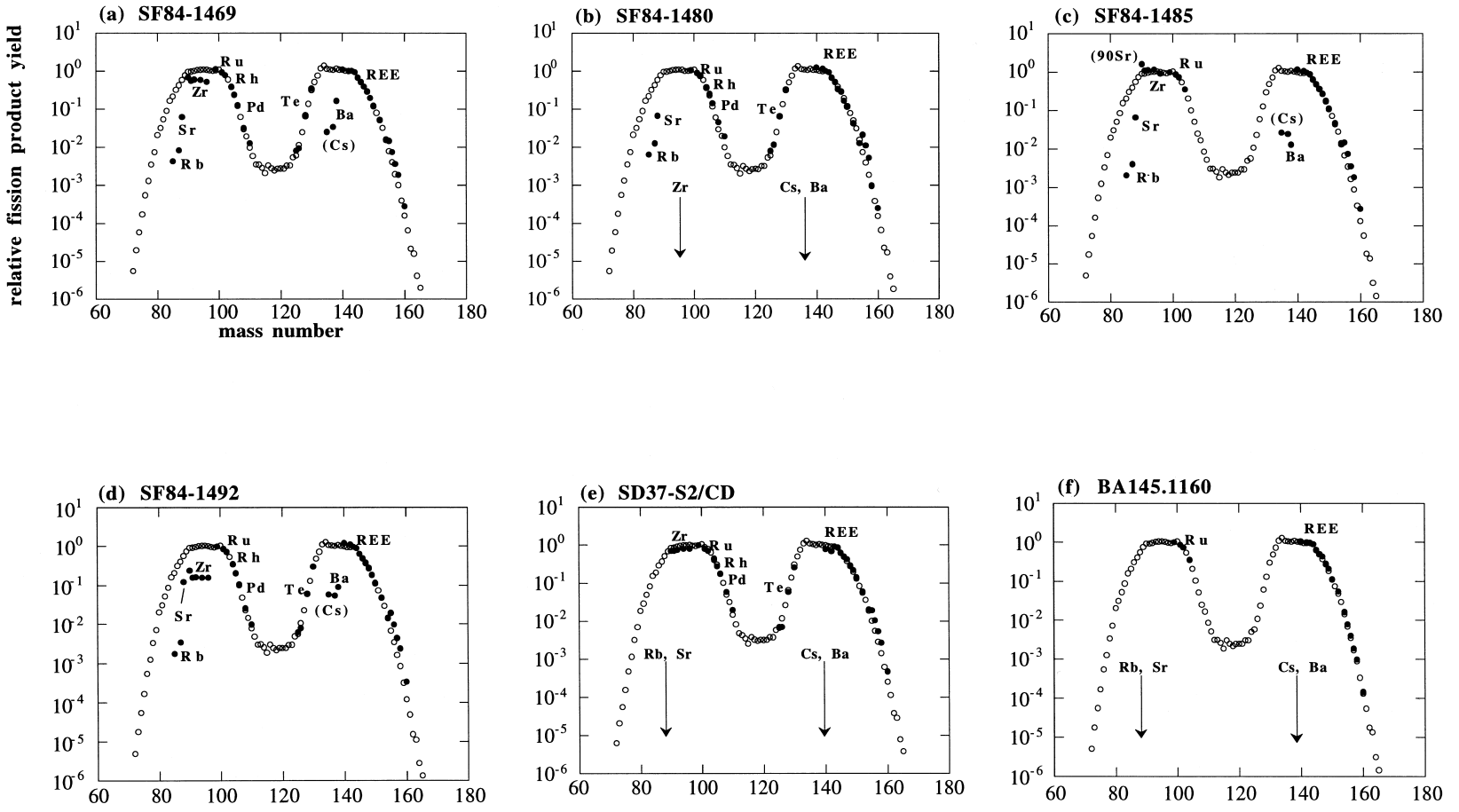

Fig. 7. Fission product yield curves of (a) 1469, (b) 1480, (c)1485, (d) 1492 from the reactor core of SF84 at RZ 10, (e) SD37-S2/CD from RZ 13, and (f) BA145.1160 from Bangombé. In each figure, closed circles indicate observed fission yield values from isotopic data. Open circles indicate expected fission yield values calculated from the experimental data by England and Rider (1988) considering the fission contribution for ^{235}U, ^{238}U, and ^{239}Pu. The fissiogenic proportions of ^{235}U, ^{238}U, and ^{239}Pu in each sample are given in Table 4.

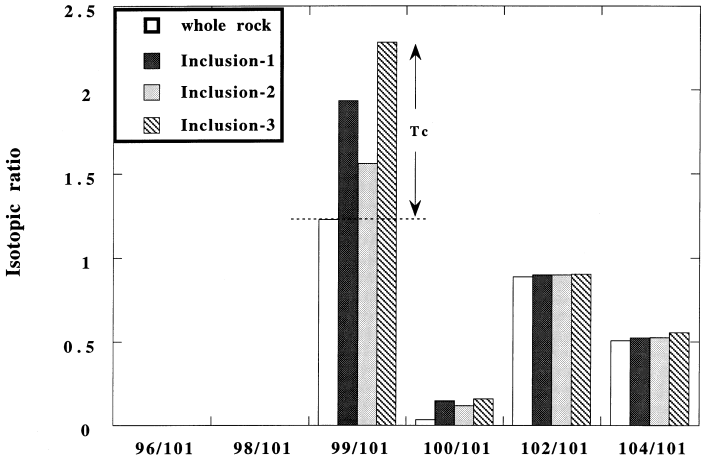

Fig. 8. Ruthenium isotopic ratios observed in whole rock sample and metallic inclusions from SD37 at RZ 13.

discussed (Hidaka et al., 1992). Curtis et al. (1989) found the partial loss of fissiogenic Nd relative to fissiogenic Te in a reactor 9 and explained it by dissolution of uraninite. Partial dissolution of uraninite grains in RZ 10 were mineralogically observed by Janeczek and Ewing (1992). As shown in Fig. 7, however, significant remobilization of fissiogenic REEs was not found in SF84 and BA145. The two curves consisting of open and closed circles in Fig. 7a,b,c,d,f are close fits with one another in the region of all REEs. This indicates good retentivities of REEs in the core. REEs are chemically compatible with U. Chemical fractionation among REEs generally occurred due to the differences in solubilities of the REE. If the uraninite grains in the reactor had been weathered under the oxidizing conditions, uraninite was dissolved and released abundant fissiogenic REEs. In the Oklo RZs, however, there are large amounts of organic matter which play an important role in covering uraninite grains and thus contain fission products (Nagy et al., 1991, 1993). Slightly negative deviations of fissiogenic La and Ce were observed in SD37 in Fig. 7e. LREEs of SD37 may have been slightly disturbed in the RZ by the thermal event associated with the intrusion of the dolerite dyke. REE isotopic studies of a series of SD37 samples along the length of the drill-core are required in order to clarify the behavior of fissiogenic LREEs due to the effect of the dolerite intrusion.

4.2.2. Ruthenium, rhodium, and palladium

Platinum group elements (PGEs) such as Ru, Rh, and Pd are so rare (less than ng/g) in common crustal rocks that the existence of fissiogenic components is easily recognized. Ruthenium cannot be distinguished between fissiogenic and natural components because it is a monoisotopic element. It can be assumed that detectable Rh in the RZs is a fissiogenic origin. Fissiogenic PGEs have good retentivities even in RZ 9 (Curtis et al., 1989, Hidaka et al., 1992). As shown in Fig. 7a–f, fissiogenic PGEs have comparably good retentivities with fissiogenic REEs in the whole rock samples of SF84, SD37, and BA145. Although fissiogenic PGEs have barely migrated out of the volume of sample (a few cm^3) used for the analyses, they have microscopically migrated and aggregated within the uraninite matrix. Similar metallic aggregates have been found in irradiated nuclear fuels. Jeffry (1967) reported the existence of fissiogenic PGE aggregates in an irradiated nuclear fuel materials. Later, Kleykamp (1985) measured the chemical compositions of the PGE aggregates. Such PGE inclusions were anticipated to exist in the Oklo RZs. Holliger (1991, 1992) first found the PGE microinclusions (ca. 100 μm of diameter) in RZs 2 and 10. In situ isotopic analysis by SIMS showed that the metallic inclusions consisted mainly of large amounts of fissiogenic PGEs.

Fissiogenic ^{99}Ru is produced from the decay of its long-lived radio precursor ^{99}Tc ($T_{1/2}$ = 2.1 x 10^5 a). Because ^{99}Tc was geochemically active during criticality of RZs, the ruthenium isotopic composition provides geochemical information on the behavior of Tc (Curtis, 1986). Chemical fractionation between Ru and Tc can be clarified by the isotopic deviation of fissiogenic ^{99}Ru. In our previous work (Hidaka et al., 1993b), we found a significant enrichment of fissiogenic ^{99}Ru relative to the other ruthenium isotopes in the PGE inclusions. In order to identify the chemical fractionation between Tc and Ru, ruthenium isotopic measurements were completed on a whole rock sample of SD37 and its metallic inclusions. The results are summarized in Fig. 8. ^{99}Ru/^{101}Ru ratios from inclusions show a large excess as compared with that from a whole rock sample. This suggests that chemical fractionation between Ru and Tc occurred while ^{99}Tc was still present. In the SD37 sample, ^{99}Tc was more mobile than Ru and was selectively incorporated into the metallic aggregates.

4.2.3. Tellurium

Tellurium is also a minor element in common rocks, although the abundances of Te in ordinary uraninite samples are higher than those of common rocks (Hidaka and Masuda, 1993). Abundant fissiogenic Te has been observed in RZs. According to isotopic studies (Curtis et al., 1989; Hidaka et al., 1992), Te is known as one of the most stable elements in RZs. Microinclusions associated with Ru, Rh, and radiogenic Pb within sulfides and arsenosulfides were observed by ion imaging using SIMS (Holliger, 1991). Judging from our isotopic measurement of Te, detectable Te in RZ samples is of only

Table 5. Comparison of tellurium isotopic compositions between measured and estimated values.

Samples	1469	1480	1492	SD.37
Measured				
$^{125}Te/^{128}Te$	0.1179 ± 7	0.1196 ± 12	0.1043 ± 11	0.1157 ± 4
$^{126}Te/^{128}Te$	0.1369 ± 4	0.1762 ± 2	0.1334 ± 4	0.1154 ± 2
$^{130}Te/^{128}Te$	5.038 ± 9	4.993 ± 18	5.173 ± 13	4.514 ± 5
Calculated				
$^{125}Te/^{128}Te$	0.0948	0.0953	0.0932	0.1003
$^{126}Te/^{128}Te$	0.1768	0.1804	0.1752	0.1811
$^{130}Te/^{128}Te$	4.908	4.911	4.986	4.633
$\Delta^{125}Te$*	+24.4 ± 0.7	+25.6 ± 1.3	+10.7 ± 1.2	+15.3 ± 0.4
$\Delta^{126}Te$	−22.6 ± 0.2	−2.3 ± 0.1	−23.9 ± 0.2	−36.3 ± 0.1
$\Delta^{130}Te$	+2.6 ± 0.2	+1.7 ± 0.4	+3.7 ± 0.3	−2.5 ± 0.1

* $\Delta^{i}Te\ (\%) = [(^{i}Te/^{128}Te)_{measured}/(^{i}Te/^{128}Te)_{calculated} - 1] \times 100$.

fissiogenic origin. However, the isotopic composition of SF84-1400, taken not from the RZ but the FA sandstone layer below the RZ, indicates a fissiogenic contribution of 11%. Although, the Te content was not measured in this sample, this measurement shows that quantities of fissiogenic Te possibly migrated from the RZ to FA layer. Among fissiogenic Te isotopes, there is a possibility that ^{125}Te and ^{126}Te had been influenced by radio-precursors ^{125}Sb ($T_{1/2}$ = 2.758 a) and ^{126}Sn ($T_{1/2}$ = 1 x 10^5 a), respectively (Loss et al., 1989). Table 5 shows a comparison of tellurium isotopic compositions between measured and calculated values. Fission product yields of Te are remarkably variable with the fission contribution rates of fissile nuclides (^{235}U, ^{238}U, and ^{239}Pu) in the RZs, because Te isotopes are located at the peak-to-valley region in the fission product yield curve. The calculated values of tellurium isotopic compositions are based on the fission inventory estimated from ruthenium isotopic compositions. A small variation observed in $\Delta^{130}Te$ is due to the difference between the retentivities of Ru and Te. The negative isotopic deviation of ^{126}Te ($-\Delta^{126}Te$ in Table 5) can be seen in SF84-1469, 1492, and SD37 samples, and only SF84-1485 has no significant depletion of fissiogenic ^{126}Te. This suggests chemical fractionation between Te and Sn. The deviation of $\Delta^{125}Te$ may be emphasized by many factors, such as the difficulty of measuring the low fission yield quantities, and uncertainties of calculated values because of the differences between the retentions of Ru and Te. Therefore, geochemical information on ^{125}Sb is based on the isotopic abundance of ^{125}Te.

4.2.4. Rubidium, strontium, cesium, and barium

The alkaline and alkali earth elements are very mobile because of their high solubilities. Until now it was difficult to find the fissiogenic Ba components in Oklo RZs because of abundant natural contamination and the low-retentivity of Ba. The range of natural Ba concentration in open pit reactors (RZs 1–9) is from 1000 to 3000 ppm (Brookins et al., 1975). On the other hand, in the SF84 reactor, the natural contamination of Ba from the environment has been suppressed and is at most 540 ppm, because this reactor has been preserved from weathering conditions. The presence of fissiogenic Rb, Sr, Cs, and Ba at the reactor SF84 series has been confirmed from the isotopic study of SF84 (Hidaka et al., 1993a; 1994). In addition, isotopic deviations of fissiogenic ^{135}Ba and ^{137}Ba provide information on the behavior of radioactive ^{135}Cs and ^{137}Cs in a RZ. According to our previous analysis of SF84 (Hidaka et al., 1993a), fissiogenic Cs (excess ^{135}Ba and ^{137}Ba) did not necessarily behave the same as fissiogenic Ba (excess ^{138}Ba). A small isotopic deviation of ^{138}Ba was observed even in the sandstone layer (SF84-1400) adjacent to RZ. Such deviations were not found in ^{135}Ba and ^{137}Ba of SF84-1400. This is an evidence for the leaking of fissiogenic Ba out of the RZ after chemical fractionation between Cs and Ba. Although isotopic measurements of Rb, Sr, and Ba in SD37 and BA145 samples were performed (see Table 2), fissiogenic components were not observed.

4.2.5. Zirconium

Among the five fissiogenic isotopes of Zr, it is noteworthy that ^{90}Zr is produced from the decay of relatively long-lived ^{90}Sr ($T_{1/2}$ = 29.1 a). Relative isotopic deviations of fissiogenic ^{90}Zr from other fissiogenic zirconium isotopic abundances indicate the retention and/or migration of ^{90}Sr in RZ10 (Hidaka et al., 1994). Fissiogenic zirconium isotope ratios and deviation factors of $^{90}Sr/^{90}Zr$ in SF84 and SD37 are shown in Table 6. SF84-1480 has little fissiogenic Zr despite enrichment of natural Zr up to 1.16 wt%, while significant amounts of fissiogenic Zr are present in SF84-1469, 1485, and 1492. No fissiogenic Zr was detected in peripheral RZ rocks, SF84-1400, 1640, and 1700. Fissiogenic Zr was disturbed in the SF84 reactor core, but Zr has not moved out of the reactor. According to the $^{90}Sr/^{90}Zr$ values shown in Table 6, observed fissiogenic ^{90}Zr in SF84-1469, 1485, and 1492 are 24–55% higher than calculated ^{90}Zr. This suggests that the excess of fissiogenic ^{90}Zr was derived from ^{90}Sr. Judging from the deviation value of $^{90}Sr/^{90}Zr$ in Table 6, SD37-S2/CD experienced little chemical fractionation between ^{90}Sr and ^{90}Zr during criticality.

4.2.6. Silver

The $^{109}Ag/^{107}Ag$ ratio in RZ is generally lower than that of the normal value ($^{109}Ag/^{107}Ag$ = 0.9220 ± .0003) by the addition of a fissiogenic component, because the fission product yield of ^{107}Ag is higher than that of ^{109}Ag. Thus, the isotopic compositions of Ag in SF84-1480, 1492, and SD37 are mixtures of fissiogenic and natural components. However, SF84-1469 has only a higher $^{109}Ag/^{107}Ag$ value ($^{109}Ag/^{107}Ag$ =

Table 6. Fissiogenic Zr in SF84 (RZ10) and SD37-S2/CD (RZ13).

Sample	$^{90}Zr/^{91}Zr$	$^{92}Zr/^{91}Zr$	$^{94}Zr/^{91}Zr$	$^{96}Zr/^{91}Zr$	Fissiogenic/total (%)	$^{90}Sr/^{90}Zr$
SF84-1469	1.21 ± 1	1.07 ± 1	1.09 ± 1	0.993 ± 5	16.0	1.24 ± 1
1480					~0	
1485	1.44 ± 1	1.05 ± 1	1.09 ± 1	0.853 ± 3	11.9	1.47 ± 1
1492	1.52 ± 1	1.05 ± 1	1.04 ± 1	1.05 ± 1	7.50	1.55 ± 1
SD37-S2/CD	0.997 ± 6	1.05 ± 1	1.21 ± 1	1.22 ± 1	71.9	1.05 ± 1

The uncertainties are given the last digit indicated.

1.0321 ± .0035) than the normal value. Fissiogenic ^{107}Ag has a long-lived radio-precursor ^{107}Pd ($T_{1/2}$ = 6.5 x 10^6 a). Because fissiogenic Pd, as well as Ru, were selectively incorporated into the micrometallic aggregates, the silver isotopic composition of SF84-1469 suggests that the high $^{109}Ag/^{107}Ag$ value was derived from chemical fractionation of Ag and Pd in the SF84. However, the loss of precursor ^{107}Pd from the Ag fraction cannot be quantitatively estimated from the silver isotopic composition alone, because fission yields of ^{107}Ag and ^{109}Ag vary with neutron energy. The interpretation of isotopic data in nuclear fission studies greatly depends upon the precise measurements of experimental fission yields as a reference, especially in the symmetric region of fission yield curve.

4.3. Distribution Profile of Fissiogenic Nuclides in SF84 Reactor Core

Elements compatible with U, such as REEs, have been relatively well retained in the reactors in spite of weathered conditions of the RZs. On the contrary there are some differences in the retention of noncompatible elements between weathered and nonweathered reactors. Besides the properties of fissiogenic nuclides, the differences in degree of retention of fissiogenic nuclides between RZs may depend upon the hydrologic, thermal, mechanical, and physicochemical conditions of the RZ. The retentivities of radionuclides vary in different parts of the same RZ. The systematic analyses of a series of samples taken from the SF84 borehole provide information on the distribution of fission products in a single reactor. Because of the fission contribution, U content, and the fact that the amount of consumed fissile nuclides are different for each sample, the comparison of the absolute amounts of fissiogenic isotopes in each sample is meaningless. In order to compare the relative amounts of fissiogenic nuclides in each sample, it is convenient to define the relative retentivity of fissiogenic nuclides. The relative retentivity is obtained from the following equation:

$$R_i = (\text{observed abundance of fissiogenic isotope (i)})/$$

$$(\text{calculated abundance (i)}) = (C_i/C_{Nd} \times (M_{Nd}/M_i) \times (Y_{Nd}/Y_i)$$

where C_i, C_{Nd} are concentrations of fissiogenic element i and ^{143}Nd, respectively. M_i, M_{Nd} are mass numbers of i and ^{143}Nd, respectively.Y_i, Y_{Nd} are fission yields of i and ^{143}Nd, respectively (England and Rider, 1988).

Thus, R_i reflects the geochemical immobility of each fissiogenic nuclide relative to fissiogenic Nd in the same sample. The relative retentivities were already applied in the study of the geochemical behavior of ^{90}Sr (Hidaka et al., 1994), ^{135}Cs and ^{137}Cs (Hidaka et al., 1993a). Including the already published data on alkaline and alkaline earth elements, distribution profiles of major fission products in SF84 are shown in Fig. 9.

The data for extinct radioisotopes, ^{90}Sr, ^{99}Tc, ^{126}Sn, and ^{137}Cs were inferred from the isotopic deficiency or excess of fissiogenic ^{90}Zr, ^{99}Ru, ^{126}Te, and ^{137}Ba, respectively. REEs have been well and homogeneously retained in the RZ, and there are no large variations among REEs. Ruthenium, rhodium, and palladium have been little disturbed in the RZ. However, as mentioned above, major Ru, Rh, and Pd have moved within grains and aggregated in the uraninite matrix. Alkaline and alkaline earth elements are greatly disturbed in the SF84 and slightly enriched near the boundary layers (1469 and 1492) rather than the vicinity of the SF84 reactor core (1480 and 1485). If the major elements formed oxide species in the RZ, oxides of alkaline and alkaline earth elements were more mobile than other major elements because of their higher reactivities with water. The profiles in Fig. 9 suggest that fissiogenic alkaline and alkaline earth elements were distributed in the core of RZ by a hydrothermal effect and moved to boundaries.

4.4. Metallic Microinclusions

As mentioned above, major fissiogenic PGEs have formed metallic microinclusions in the uraninite grains of RZs 10 and 13 (Holliger, 1991, 1992). According to in situ analysis by an electron probe microanalyzer (EPMA), the inclusions mainly consist of chalcophile elements such as Pb, Ru, and Rh (see Table 7a). In the case of ordinary terrestrial crustal rocks, such minerals including platinum group elements in ultrabasic rocks (Peck and Keays, 1990; Nixon et al., 1990; Nilsson, 1990). On the other hand, the metallic inclusions found in the Oklo reactor core consist of fission-produced chalcophile elements. As shown in the isotopic data of Table 7b, Ru in the micrometallic aggregates is purely fissiogenic because no ^{96}Ru and ^{98}Ru isotopes are detected. Ruthenium is mostly produced by fission, and a large part of the fissiogenic Ru is incorporated into metallic inclusions. Lead is also one of major elements in the inclusion. Judging from the stoichiometric compositions of metallic inclusions, originally existing PbS might have helped to aggregate the fissiogenic PGEs and formed such unique inclusions in RZ.

4.5. Actinide Abundances

^{232}Th and ^{209}Bi were produced by the decay of nucleogenic actinides in the RZs. Therefore, Th and Bi can be used as possible tracers to investigate the behaviours of some actinides.

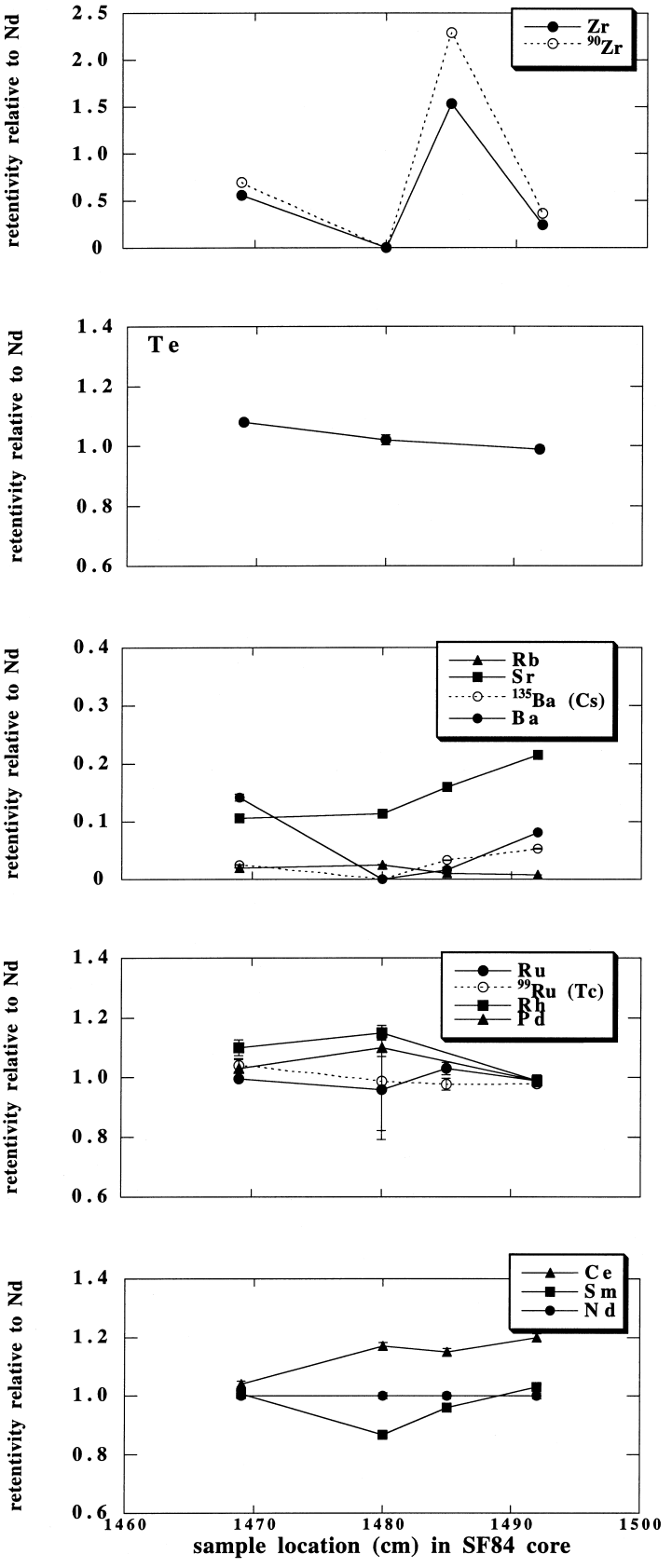

Fig. 9. Distribution profiles of major fission products in SF84.

Table 7. Metallic inclusions of reactor core samples from SF29-9166 (zone 10) and SD.37-S2/CD (zone 13).

(a) Chemical composition (wt%)

	Pb	Ru	Rh	Te	U	As	S	Total
SF29-1	22.03	23.12	4.57	1.00	0.56	31.63	12.87	95.78
2	28.22	18.12	3.75	0.62	0.61	25.11	19.44	95.87
3	21.14	25.83	3.13	0.30	0.68	30.92	13.77	95.77
4	14.16	31.79	6.64	0.47	3.73	35.20	3.94	95.93
5	16.98	26.42	5.05	1.13	1.51	34.08	8.07	93.24
SD37-1	54.09	23.49	3.48	1.85	0.00	4.40	9.62	96.93
2	43.69	30.89	4.88	1.90	0.23	7.02	7.91	96.52
3	40.63	31.78	6.23	3.61	0.35	7.81	7.31	97.72
4	38.44	37.02	5.13	2.51	0.27	5.31	6.75	95.43
5	46.59	26.69	4.29	2.77	0.09	8.53	8.86	97.82

The uncertainties of the analytical values are 0.6–0.8% for Pb, Ru, As and S, 1.5–2.0% for Rh and Te, and 3.5–7.0% for U.

(b) Isotopic composition of Ru (atom %)

	^{96}Ru	^{98}Ru	^{99}Ru	^{100}Ru	^{101}Ru	^{102}Ru	^{104}Ru
SF29-1	<0.01	<0.01	23.71	1.21	30.72	27.37	16.99
2	<0.01	<0.01	23.81	1.16	30.25	26.90	17.88
SD37-1	<0.01	<0.01	42.94	3.30	22.20	19.95	11.61
2	<0.01	<0.01	38.06	2.90	24.38	21.87	12.78
3	<0.01	<0.01	46.62	3.22	20.41	18.41	11.33
STD*	5.54	1.86	12.74	12.60	17.05	31.57	18.66
Fission**							
^{235}U	—	—	34.97	—	29.66	24.60	10.76
^{238}U	—	—	25.91	—	25.99	27.00	21.10
^{239}Pu	—	—	25.44	—	24.64	25.02	24.90

* STD means the value of terrestrial standard materials.
** The fission data are from England and Rider (1988).
The data of chemical compositions for SF29-1~5 and ruthenium isotopic compositions for SD37-1~3 are from Hidaka et al. (1993b).

One cannot directly distinguish the nucleogenic and primordial Th and Bi by an isotopic study, because both of these elements are monoisotopic elements. However, the nucleogenic amounts of actinides in the RZs can be calculated by using nuclear parameters (Fréjacques et al., 1975). Therefore, possibility of distributions of nucleogenic actinides in the RZs would be discussed from the comparison with measured and calculated contents of Th and Bi.

4.5.1. ^{232}Th from ^{236}U and ^{240}Pu

As shown in samples SF84-1640 and 1700, the Th content of the RZ is generally low. Most of the ^{232}Th in the RZs is produced from the α decay of ^{240}Pu after two successive neutron capture reactions of ^{238}U and from the a decay of ^{236}U after neutron capture of ^{235}U:

$$^{238}\mathrm{U}(\mathrm{n}, \gamma 2\beta)^{239}\mathrm{Pu},\ ^{239}\mathrm{Pu}(\mathrm{n}, \gamma)^{240}\mathrm{Pu}$$

$$^{235}\mathrm{U}(\mathrm{n}, \gamma)^{236}\mathrm{U}$$

The amount of Th produced by the above nuclear reactions can be estimated from the conventional method using nuclear parameters and U data (Fréjacques et al., 1975). On the basis of the Fréjacques et al. (1975) method, the abundances of secondarily produced Th were calculated. Table 8 shows a comparison of Th contents in RZ samples between calculated and measured values. The calculated Th content in each sample is not necessarily in good agreement with the measured value. Measured Th data of 1480 and 1485 are 50% lower than those of the calculated data, while measured values in 1469 and 1492 are 25~50% higher than those of the calculated values. The distribution profile of Th relative to U (Th/U) in the SF84 core is shown in Fig. 10. Considering the half lives of ^{236}U (2.34×10^7 a) and ^{240}Pu (6.57×10^3 a), nucleogenic Th in the RZ might have behaved more like U than Pu. However, if chemical fractionation between Pu and U had occurred at the early stage of reactor operation, secondary-produced Th might have behaved more like Pu than U. Figure 10 suggests that Th was distributed from the vicinity of RZ to the boundary in SF84. Assuming that all the Th content in SF84-1400 is nucleogenic origin, one can understand that Th has been removed from the vicinity of reactor core to the boundary, and moreover, into the FA layer. Considering the low Th content in SF84-1640 and 1700 (FB pelite), it is reasonable that abundant Th in SF84-1400 (FA sandstone) might have formed from the decay of ^{240}Pu. Fréjacques et al. (1975) compared measured Th contents with calculated ones and noted the good retention of nucleogenic Th relative to U in the SC-36 samples at RZ 2. RZ 10, including SF84, has been preserved due to the limited alteration, because RZ 10 is located at a depth of 400 m from the surface. On the other hand, RZ 2 has been exposed to an oxidizing atmosphere for a longer time than RZ 10, because it is located near the surface. There is a possibility that Th and U of SC-36 have been redistributed and homogenized by secondary alteration and that the fine-scale distribution profiles of Th/U that appeared in SF84 could not be observed in SC-36.

SD37-S2/CD, taken from the vicinity of the RZ 13, is en-

Table 8. Elemental abundances of nucleogenic thorium and bismuth.

(a) Th

Sample	U content (wt. %)	Calculated from ^{238}U*	$^{232}Th/^{238}U$ (ppm) from ^{235}U**	Calculated Th (ppm)	Measured Th (ppm)
SF84-1469	17.2 ± 2	412	2669	517 ± 8	805 ± 12
1480	7.06 ± 7	352	3713	280 ± 4	168 ± 4
1485	14.9 ± 1	365	3055	497 ± 12	253 ± 5
1492	24.3 ± 3	283	2805	732 ± 11	918 ± 9
SD37	59.4 ± 6	354	3482	2221 ± 23	3588 ± 37
BA145-1160	45.0 ± 4	403	1634	893 ± 35	607 ± 9

The uncertainties are given the last digit indicated.
* Produced from the neutron capture of ^{238}U (see text).
** Produced from the neutron capture of ^{235}U (see text).

(b) Bi

Sample	U content (wt. %)	Calculated from ^{236}U*	$^{237}U/^{238}U$ (ppm) from ^{238}U**	Calculated Bi (ppm)	Measured Bi (ppm)
SF84-1469	17.2 ± 2	102	65	25.2 ± 4	21.7 ± 7
1480	7.06 ± 7	128	98	14.0 ± 2	6.55 ± 14
1485	14.9 ± 1	108	77	24.2 ± 6	4.50 ± 9
1492	24.3 ± 3	92.8	70	34.7 ± 5	23.6 ± 6
SD37	59.4 ± 6	345	96	230 ± 2	463 ± 5
BA145-1160	45.0 ± 4	61.3	38	39.2 ± 15	12.0 ± 5

The uncertainties are given the last digit indicated.
* Produced from the neutron capture of ^{236}U (see text).
** Produced from the (n, $2n$) reaction of ^{238}U (see text).

riched by a large amount of Th (3588 ppm). The measured Th content of SD37-S2/CD, 3588 ppm, is significantly larger than those of other RZ samples (168–918 ppm). SD37 is characterized as an uncommon RZ with a short criticality duration (2.42 x 10^4 a) and a high neutron fluence (7.8 x 10^{20} n/cm^2) as shown in Table 4. The higher neutron flux in SD37 might have produced significant amounts of ^{240}Pu and ^{236}U in the reactor core. Detailed distribution profiles of Th in SD37 and BA145 could not be provided because only a single measurement from each RZ was made.

4.5.2. ^{209}Bi from ^{237}Np

In the RZs, ^{209}Bi was produced by the decay of ^{237}Np. Primordial ^{237}Np is now an extinct radionuclide, and it is produced mainly by the following reactions:

$$^{235}U(n, \gamma)^{236}U, \ ^{236}U(n, \gamma\beta)^{237}Np$$

$$^{238}U(n, 2n\beta)^{237}Np$$

$$^{238}U(n, \gamma 2\beta)^{239}Pu, \ ^{239}Pu(n, \gamma)^{240}Pu, \ ^{240}Pu(n, \gamma\beta\alpha)^{237}Np$$

^{237}Np has a long half-life ($T_{1/2}$ = 2.1 x 10^6 a) and finally decays to stable ^{209}Bi via long-lived ^{233}U ($T_{1/2}$ = 1.6 x 10^5 a). Considering the estimated operation time of the RZs is less than the half life of ^{237}Np (see Table 4), the ^{237}Np produced by the above reactions was still present during reactor operation.

Low Bi contents of SF84-1400, 1640, and 1700 samples confirm that the RZs contained little primordial Bi, and all of detectable Bi in the RZ samples are the decay products from ^{237}Np. The profile of Bi/U in the SF84 is shown in Fig. 10. Fréjacques et al. (1975) found significant differences between calculated $^{209}Bi/^{238}U$ and measured values and suggested the possibility of migration of ^{237}Np in reactor zone 2 (SC36 samples). According to their estimate, the loss of ^{209}Bi was up to 30% at its maximum in the same reactor core samples. Relatively large difference between calculated and measured ^{209}Bi abundances are found, especially around the center of RZ (1480 and 1485) rather than near the boundaries (1469 and 1492). Our results shown in Fig. 10 suggest that the thermal distribution of ^{209}Bi had occurred in the SF84 core. As described previously, most of fission products are well preserved in the SF84 core. Even remarkably mobile fission products, such as Sr and Ba, still remain in the core. One cannot simply conclude that the abundance pattern of Bi/U reflects the distribution of Np in the SF84 core, because there is the possibility that Bi itself has been redistributed after complete decay of Np. Considering the similarity of chemical properties between Pb and Bi, the redistribution behaviour of Bi itself may have been deduced from that of Pb. According to the mineralogical observations of RZ samples made by Janeczek and Ewing (1995), radiogenic Pb was released from uraninite by thermally-induced diffusion. These Pb data suggest that the secondary-produced Bi had been possibly redistributed in the SF84 reactor core. However, judging from the lack of enrichment of Bi in peripheral rocks of the RZ, Bi has been preserved in the RZ.

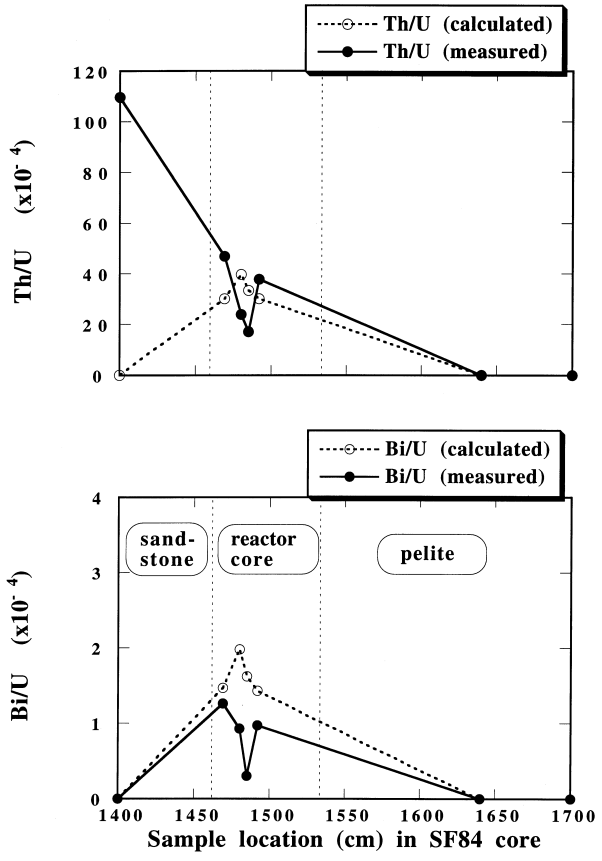

Fig. 10. Th/U and Bi/U relative abundance patterns of SF84. Closed and open circles in the figures indicate measured and calculated values, respectively (see text).

Bismuth as well as Thorium has been enriched in SD37-S2/CD. A large amount of ^{237}Np might have been produced under the condition of high neutron flux in SD37.

4.6. Performance Assessment on the Behaviour of Fissiogenic Elements in RZs

The isotopic results obtained from RZs 10 and 13 at Oklo and from Bangombé have generated data which are useful in understanding the geochemical behaviour of fissiogenic nuclides. The characteristics of the geochemical mobility of these fissiogenic elements as obtained in this study are summarized in Table 9. Using the descriptions made in previous studies (Jeffry, 1967; Ruffenach et al., 1980; Gauthier-Lafaye et al., 1996), the main fission products are classified into five groups. (1) Soluble and homogeneously distributed elements in the UO_2: REE have been well reserved in most RZs, but light REEs such as La and Ce have been partially removed out of RZs 1–9. (2) Formation of metallic aggregates in the UO_2: Ru, Tc, Rh, Pd, and Te formed a metallic phase and have been well retained in RZs. (3) Low solubility elements in the UO_2 and largely fractionated from UO_2 matrix: Rb, Sr, and Ba have been almost lost in many RZs, but 1–10% of fissiogenic fractions have been retained in the little weathered RZ portion, SF84. (4) Highly soluble elements: Cs as well as another alkaline element Rb has almost disappeared in many RZs, but estimated Cs from the excess of fissiogenic ^{135}Ba and ^{137}Ba in SF84 has been slightly retained around the boundaries between RZ and wall rock layers. (5) Gaseous elements: Kr and Xe have been lost to a great extent in RZs 1–9, but not analysed in this study.

5. CONCLUSIONS

Isotopic measurements by mass spectrometry provided the useful information of geochemical and neutronic characteristics of the reactors SF84 (RZ 10), SD37 (RZ 13), and BA145 (Bangombé). The migration or retention behaviour of fission products in the SF84 borehole was obtained from the systematic isotopic analyses. In addition, judging from the distribution profiles of nuclear parameters, such as neutron fluence, restitution factor of ^{235}U, neutron spectrum index, U content, and U

Table 9. Geochemical behavior of fission products.

	Irradiated UO_2*	Oklo RZ 1~9	Oklo SF84 (RZ 10)	Oklo SD37 (RZ 13)	Bangombé BA145
Non-volatile					
REEs	Homogeneously distributed in the matrix	Partial release of LREEs	Well-retained in the reactor	Well-retained in the reactor	Well-retained in the reactor
Ru, Tc, Pd, Te	Metallic inclusions along the grain boundaries	Well-retained in the reactor Unidentification of metallic inclusions	Well-retained in the reactor Formation of metallic inclusions in the matrix	Well-retained in the reactor Formation of metallic inclusions in the matrix	Well-retained in the reactor Formation of metallic inclusions**
Volatile					
Ba, Sr, Rb	Oxide inclusions within the matrix	Almost disappeared	1~10% of fission products around the boundaries between RZ and sandstones	Almost disappeared	Almost disappeared
Cs	Solid phase in cooler region of the matrix	Almost disappeared	1~10% of fission products around the boundaries between RZ and sandstones	Almost disappeared	Almost disappeared
Gaseous					
Kr, Xe	Bubbles within grains	Almost disappeared	Not analysed	Not analysed	Not analysed

* The data from Jeffry (1967) and Kleykamp (1985).
** The data from Janeczek (pers. commun.).

isotopic ratio in the SF84 core, the operating characteristics of natural fission reactors are largely associated with the ambient geological conditions at the time of criticality. The reactor core of the borehole SF84 of RZ 10 behaves as a relatively closed-system as regards its fission product retention, and most of the fission products, such as the REEs, have been well protected from any alteration during past 2 billion years. Unlike RZs 1–9, the fissiogenic alkaline and alkaline earth elements are still present in a certain degree of retention in this RZ. Nuclear parameters estimated from the isotopic results suggests that SD37 is an uncommon reactor and the duration of its criticality was five to ten times shorter than the other reactors. BA145 has a similar nuclear characteristic to the common reactors such as SF84, although its reactor core is very thin.

The final goal of this study is to apply the geochemical data obtained from natural reactors to the performance assessment of a geological repository for radioactive waste. The retentivities of fission products produced in RZs vary in the different kinds of RZs, because retentions greatly depend upon the geological setting, such as weathering history and the occurrence of hydrothermal events after the criticality. We detected fissiogenic Rb, Sr, and Ba from the little weathered RZ samples, and the mobilities of ^{135}Cs could be estimated from the isotopic deviations of ^{135}Ba. If we are to resolve the issue on nuclear waste storage more clearly from the viewpoint of a natural analogue study, highly precise and in situ isotopic observations of various mineral species in RZ samples are essential for understanding the release or retention of fission products. As identification of the existence of fissiogenic PGE aggregates can be carried out by in situ ion observation, it is expected that other tiny inclusions consisting of fission products such as Ba, Sr, and Rb oxides may be detected by sensitive and high resolution in situ isotopic analysis.

Acknowledgments—We are indebted to Oklo Working Group organized by CEC and CEA for providing samples. We would like to thank Drs. P. L. Blanc (CEA), F. Gauthier-Lafaye (CNRS), and H. von Maravic (CEC) for their devoted cooperation for the Working Group. A constructive review by Prof. R. C. Ewing (Univ. of Michigan) was of great help in the improvement of this manuscript. Journal reviews from Dr. R. D. Loss (Curtin Univ. of Tech.) and Prof. J. Janeczek (Univ. of Silesia) were very helpful. This study was financially supported in a part by a Grant-in-Aid for Scientific Research of Ministry of Education, Science and Culture, Japan (Nos. 06640637 and 07640659 to H.H.).

REFERENCES

Bodu R., Bouzigues H., Morin N., and Pfiffelmann J. P. (1972) Sur l'existence d'anomalies isotopiques rencontrées dans l'uranium du Gabon. *C.R. Acad. Sci. Paris* **275**, 1731-1734.

Brookins D. G., Lee M. J., Mukhopadhyay B., and Bolivar S. L. (1975) Search for fission-produced rubidium, strontium, cesium, and barium at Oklo. *Proc. Oklo Phenomenon*, 401–413. IAEA.

Bros R., Turpin L., Gauthier-Lafaye F., Holliger P., and Stille P. (1993) Occurrence of naturally enriched ^{235}U: Implications for plutonium behaviour in natural environments. *Geochim. Cosmochim. Acta* **57**, 1351–1356.

Bros R., Gauthier-Lafaye F., Larqué P., Samuel J., and Stille P. (1994) Mobility of uranium, thorium, and lanthanides around the Bangombé natural nuclear reactor (Gabon). *Proc. XVIII Intl. Symp. Sci. Basis Nucl. Waste Management* , 1187–1194.

Burns P. C., Ewing R. C., and Miller M. L. (1997) Incorporation mechanisms of actinide elements into the structures of U^{6+} phases formed during the oxidation of spent nuclear fuel. *J. Nucl. Mater.* **245**, 1–9.

Chen J. H. and Wasserburg G. J. (1981) Isotopic determination of uranium in picomole and subpicomole quantities. *Anal. Chem.* **53**, 2060–2067.

Curtis D. B. (1986) Geochemical controls on ^{99}Tc transport and retention. *Chem. Geol.* **55**, 227–231.

Curtis D. B. et al. (1989) Fission product retention in the Oklo natural fission reactors. *Appl. Geochem.* **4**, 49–62.

DeLaeter J. R., Rosman K. J. R., and Smith C. L. (1980) The Oklo natural reactor: Cumulaive fission yields and retentivity of the symmetric mass region fission products. *Earth Planet. Sci. Lett.* **50**, 238–246.

England T. R. and Rider B. F. (1988) Chainy for MITO-TAL. Los Alamos Rpt. LA-UR-88-1696.

Eugster O., Tera F., and Wasserburg G. J. (1969) Isotopic analyses of barium in meteorites and in terrestrial samples. *J. Geophys. Res.* **74**, 3897–3908.

Eugster O., Tera F., Burnett D. S., and Wasserburg G. J. (1970) Isotopic composition of gadolinium and neutron-capture effects in some meteorites. *J. Geophys. Res.* **75**, 2753–2768.

Faure G. and Powell J. L. (1972) *Strontium Isotope Geology*. Springer Verlag.

Fréjacques C., Blain C., Devillers C., Hagemann R., and Ruffenach J. C. (1975) Conclusions tirees de l'etude de la migration des produits de fission. *Oklo Phenomenon*, 509–524. IAEA.

Gauthier-Lafaye F. (1995) Géologie des réacteurs. Etude des épontes et des transferts anciens. Rept. CEA-CEC. Contract CEC No. F112W-CT91-0071.

Gauthier-Lafaye F. and Weber F. (1989) The Francevillian (lower Proterozoic) uranium ore deposits of Gabon. *Econ. Geol.* **84**, 2267–2285.

Gauthier-Lafaye F., Weber F., and Ohmoto H. (1989) Natural fission reactors of Oklo. *Econ. Geol.* **84**, 2286–2295.

Gauthier-Lafaye F., Holliger P., and Blanc P.-L. (1996) Natural fission reactors in the Franceville basin, Gabon: A review of the conditions and results of a critical event in a geological system. *Geochim. Cosmochim. Acta* **60**, 4831–4852.

Hagemann R. and Roth E. (1978) Relevance of the studied of the Oklo natural reactors to the storage of radioactive wastes. *Radiochim. Acta* **25**, 241–247.

Hagemann R., Devillers C., Lucas M., Lecomte T., and Ruffenach J. C. (1975) Estimation de la duree de la reaction: Limitations imposées par les données neutroniques. *Proc. Oklo Phenomenon*, 415–423. IAEA.

Hidaka H. and Masuda A. (1988) Nuclide analyses of rare earth elements of the Oklo uranium ore samples: A new method to estimate the neutron fluence. *Earth Planet. Sci. Lett.* **88**, 330–336.

Hidaka H. and Masuda A. (1993) Isotopic search for spontaneous fission-produced ruthenium, silver, and tellurium in uraninite. *Chem. Geol.* **106**, 187–195.

Hidaka H., Masuda A., Fujii I., and Shimizu H. (1988) Abundance of fissiogenic and pre-reactor natural rare-earth elements in a uranium ore sample from Oklo. *Geochem. J.* **22**, 47–54.

Hidaka H., Kano N., and Masuda A. (1991) Estimation of burnup in the Oklo natural nuclear reactor from ruthenium isotopic composition. *J. Radioanal. Nucl. Chem. Lett.* **155**, 107–113.

Hidaka H., Konishi T., and Masuda A. (1992) Reconstruction of cumulative fission yield curve and geochemical behaviors of fissiogenic nuclides in the Oklo natural reactors. *Geochem. J.* **26**, 227–239.

Hidaka H., Holliger P., and Masuda A. (1993a) Evidence of fissiogenic cesium estimated from barium isotopic deviations in an Oklo natural reactor zone. *Earth Planet. Sci. Lett.* **114**, 391–396.

Hidaka H., Shinotsuka K., and Holliger P. (1993b) Geochemical behaviour of ^{99}Tc in the Oklo natural fission reactors. *Radiochim. Acta* **63**, 19–21.

Hidaka H., Sugiyama T., Ebihara M., and Holliger P. (1994) Isotopic evidence for the retention of ^{90}Sr inferred from excess ^{90}Zr in the Oklo natural fission reactors: Implication for geochemical behaviour of fissiogenic rubidium, strontium, cesium, and barium. *Earth Planet. Sci. Lett.* **122**, 173–182.

Holliger P. (1988) In situ U-Pb ages on uranium oxides using ion

microprobe: methodology and geochemical implications. *C.R. Acad. Sci. Paris* **307** (Ser. II), 367–373.

Holliger P. (1991) Systematique U-Pb et etude isotopique in situ ^{235}U-produits de fission de la zone de reaction hybride SF29 (zone 10): Autres zones d'interet sur le site d'Oklo pour les etudes futures. CEA-DTA-CENG, Note Technique DEM No. 18/91.

Holliger P. (1992) Les nouvelles zones de réaction d'Oklo: Datation U-Pb et caractérisation in situ des produits de fission à l'analyseur ionique. CEA-DTA-CENG, Note Technique DEM No. 01/92.

Holliger P. (1993a) Oklo-terme source: Paramètres nucléaires. Etude isotopique et topographie de la zone de reaction 10. CEA-DTA-CENG, Note Technique DEM No. 93/96.

Holliger P. (1993b) SIMS studies on the Oklo natural fission reactors. Invited lecture. *Proc. SIMS IX Conf.* , 8–12.

Holliger P. (1994) Terme source: Caractérisation isotopique, paramètres nucléaires et modélisation. CCE Report FI12W-CT91-0071. Prog. Oklo -Analogues Naturels.

Holliger P. and Devillers C.(1981) Contribution à l'étude de la température dans les réacteurs fossiles d'Oklo par la mesure du rapport isotopique du lutétium. *Earth Planet. Sci. Lett.* **52**, 76–84.

I.A.E.A. (International Atomic Energy Agency) (1975) SM-204: Le phénomène d'Oklo. Proc. Tech. Comm. STI/PUB/405.

I.A.E.A. (International Atomic Energy Agency) (1978) TC-119: Natural Fission Reactors. Proc. Tech. Comm. STI/PUB/475.

Janeczek J. and Ewing R. C. (1992) Dissolution and alteration of uraninite under reducing conditions. *J. Nucl. Mater.* **190**, 157–173.

Janeczek J. and Ewing R. C. (1995) Mechanisms of lead release from uraninite in the natural fission reactors in Gabon. *Geochim. Cosmochim. Acta* **59**, 1917–1931.

Janeczek J. and Ewing R. C. (1996) Florencite-(La) with fissiogenic REEs from a natural fission reactor at Bangombé, Gabon. *Amer. Mineral.* **81**, 1263–1269.

Jeffry B. M. (1967) Microanalyses of inclusions in irradiated UO_2. *J. Nucl. Mater.* **22**, 33–40.

Kleykamp K. (1985) The chemical state of fission products in oxide fuels. *J. Nucl. Mater.* **131**, 221–246.

Lingenfelter R. E., Canfield E. H., and Hampel V. E. (1972) The lunar neutron flux revisited. *Earth Planet. Sci. Lett.* **16**, 355–369.

Loss R. D., Rosman K. J. R., and DeLaeter J. R. (1983) Measurement of silver, tellurium, and lead in geochemical reference materials by mass spectrometric isotope-dilution analysis. *Talanta* **30**, 831–835.

Loss R. D., Rosman K. J. R., and DeLaeter J. R. (1984) Transport of symmetric mass region fission products at the Oklo natural reactors. *Earth Planet. Sci. Lett.* **68**, 240–248.

Loss R. D. et al. (1988) The Oklo natural reactors: Cumulative fission yields and nuclear characteristics of Reactor Zone 9. *Earth Planet. Sci. Lett.* **89**, 193–206.

Loubet M. and Allegre C. J. (1977) Behavior of the rare earth elements in the Oklo natural reactor. *Geochim. Cosmochim.. Acta* **41**, 1539–1548.

Maas R. and McCulloch M. T. (1990) A search for fossil nuclear reactors in the Alligator River Uranium Field, Australia: Constraints from samadium, gadolinium, and neodymium isotopic studies. *Chem. Geol.* **88**, 301–315.

Masuda A., Hirata T., and Shimizu H. (1986) Determinations of osmium isotope ratios in iron meteorites and iridosmines by ICP-MS. *Geochem. J.* **20**, 233–239.

Menet C., Menager M.-T., and Petit J.-C. (1992) Migration of radioelements around the new nuclear reactors at Oklo: Analogies with a high-level waste repository. *Radiochim. Acta* **58/59**, 395–400.

Minster J. F. and Allegre C. J. (1981) The isotopic composition of zirconium in terrestrial and extraterrestrial samples: Implications for extinct ^{92}Nb. *Geochim. Cosmochim. Acta* **46**, 565–573.

Nagy B. et al. (1991) Organic matter and containment of uranium and fissiogenic isotopes at the Oklo natural reactors. *Nature* **354**, 472–475.

Nagy B., Gauthier-Lafaye F., Holliger P., Mossman D. J., Leventhal J. S., and Rigali M. J. (1993) Role of organic matter in the Proterozoic Oklo natural fission reactors, Gabon, Africa. *Geology* **21**, 655–658.

Naudet R. (1991) *Oklo: des réacteurs nucléaires fossiles.* Comm. Energie Atomique Paris.

Neuilly M., Bussac J., Fréjacques C., Nief G., Vendryes G., and Yvon J. (1972) Sur l'existence dans un passé reculé d'une réaction en chaîne naturelle de fission, dans le gisement d'uranium d'Oklo (Gabon). *C.R. Acad. Sci. Paris* **275**, 1847–1849.

Nilsson L. P. (1990) Platinum-group mineral inclusions in chromitite from the Osthammeren ultramafic tectonite body, south-central Norway. *Mineral. Petrol.* **42**, 249–263.

Nixon G. T., Cabri L. J., and Laflamme J. H. G. (1990) Platinum-group-element mineralization in lode and placer deposits associated with the Tulameer Alaskan-type complex, British Columbia. *Canadian Mineral.* **28**, 503–35.

Peck D. C. and Keays R. R. (1990) Geology, geochemistry, and origin of platinum-group-element-chromite occurrences in the Heazlewood River Complex, Tasmania. *Econ. Geol.* **85**, 765–793.

Roth E. (1977) The discovery and study of the nuclear reactor in Oklo. *J. Radioanal. Chem.* **37**, 65–78.

Ruffenach J. C., Menes J., Devillers C., Lucas M., and Hagemann R. (1976) Etudes chimiques et isotopiques de l'uranium, du plomb et de plusieurs produits de fission dans un echantillon de minerai du reacteur naturel d'Oklo. *Earth Planet. Sci. Lett.* **30**, 94–108.

Ruffenach J. C., Hagemann R., and Roth E. (1980) Isotopic abundances measurements a key to understanding the Oklo phenomenon. *Z. Naturforsch.* **35a**, 171–179.

Toulhoat P. et al. (1994) Preliminary studies of groundwater flow and migration of uranium isotopes around the Oklo natural reactors. *Radiochim. Acta* **66/67**, 351–358.